

Relay Selection for Simultaneous Information Transmission and Wireless Energy Transfer: A Tradeoff Perspective

Diomidis S. Michalopoulos, *Member, IEEE*, Himal A. Suraweera, *Member, IEEE*,
and Robert Schober, *Fellow, IEEE*

Abstract

In certain applications, relay terminals can be employed to simultaneously deliver information and energy to a designated receiver and a radio frequency (RF) energy harvester, respectively. In such scenarios, the relay that is preferable for information transmission does not necessarily coincide with the relay with the strongest channel to the energy harvester, since the corresponding channels fade independently. Relay selection thus entails a tradeoff between the efficiency of the information transfer to the receiver and the amount of energy transferred to the energy harvester. The study of this tradeoff is the subject on which this work mainly focuses. Specifically, we investigate the behavior of the ergodic capacity and the outage probability of the information transmission to the receiver, for a given amount of energy transferred to the RF energy harvester. We propose two relay selection methods that apply to any number of available relays. Furthermore, for the case of two relays, we develop the optimal relay selection method in a maximum capacity / minimum outage probability sense, for a given energy transfer constraint. A close-to-optimal selection method that is easier to analyze than the optimal one is also examined. Closed-form expressions for the capacity-energy and the outage-energy tradeoffs of the developed schemes are provided and corroborated by simulations. Interesting insights on the aforementioned tradeoffs are obtained.

Index Terms

Capacity-energy tradeoff, energy harvesting, ergodic capacity, relay selection, outage probability, wireless energy transfer.

D. S. Michalopoulos and R. Schober are with the Department of Electrical and Computer Engineering, University of Erlangen-Nuremberg, Germany, (e-mail: {michalopoulos, schober}@int.de)

H. A. Suraweera is with the Singapore University of Technology and Design, 20 Dover Drive, Singapore 138682 (e-mail: himalsuraweera@sutd.edu.sg).

I. INTRODUCTION

The approach towards energy consumption in communication systems has experienced a drastic change in the last few years. The enormous growth of telecommunication networks has led to a massive increase of their energy consumption. Forecasts on the energy consumption of future applications place information and communication technology (ICT) networks among the big energy consumers, so that the energy consumed by ICT infrastructure worldwide is anticipated to reach the current level of the total global electricity consumption in the next 20-25 years [1], [2]. Hence, owing to this growing concern regarding the energy footprint of communications, modern architectures consider energy not as an unlimited resource, as it traditionally was, but as a scarce resource which plays a significant role in system design [3], [4].

In line with the contemporary trend towards renewable sources, energy harvesting appears as a viable solution to powering wireless communications nodes [5]–[7]. In addition, energy harvesting offers wireless communication substantial flexibility, since wireless nodes are not necessarily attached to a fixed power supply nor are they dependent on battery replacement and/or recharge [6]. The most common forms of harvested energy used in wireless communications are solar energy, piezoelectric energy, and energy harvested from radio frequency (RF) transmissions [8]–[10]. The latter form attracts particular interest as it allows terminals with low energy requirements to be remotely powered, thereby it provides a feasible solution for cases where remote energy supply is the only powering option (for example, in body area networks where devices are implanted into the human body such that accessing them is impossible) [11]. Moreover, as information and energy are transmitted via the same signal, RF energy harvesting poses challenges on the efficient design of systems that provide simultaneous information and energy transfer to the same terminal [12]–[15] or to different terminals [16]–[18].

Motivation: Relay-assisted communication and particularly relay selection offers a substantial improvement to the quality of service in wireless networks, particularly in scenarios where source and destination are located far apart from one another [19], [20]. Naturally, the same concept applies also to wireless energy transfer scenarios, as the large path-loss of the energy-bearing channel renders wireless energy transfer over large distances prohibitive. In this regard, suppose that relay terminals are used both for assisting the information transmission to a designated receiver and the energy transfer to a designated RF energy harvester, which are located far from each other.

Then, the question that arises is which relay to activate in each transmission session, as the activated relay will provide the receiver and the harvester with data and energy respectively and the channels used for information and energy transfer vary independently from each other. Since the relay that provides the most efficient data transmission to the receiver does not necessarily coincide with the relay that provides the largest energy transfer to the RF harvester, a tradeoff is revealed: The quality of the information transmission to the receiver is exchanged for the efficiency of the energy transfer to the harvester. This tradeoff is reflected in the decision on which relay is selected, and represents the main topic of interest of this work.

Contribution: We show via mathematical and numerical analysis that, depending on the application scenario and the available amount of channel state information (CSI), the achievable tradeoff can range from a linear exchange between data and energy transmission to the optimal feasible tradeoff. In particular, our results can be summarized as follows. For the versatile scenario where N relays are available for information forwarding and wireless energy transfer, we study two relay selection schemes, namely the time-sharing and the threshold-checking scheme, in terms of the achievable tradeoff between average energy transfer and ergodic capacity, as well as the tradeoff between energy transfer and outage probability. For the case where two relays are available ($N = 2$), we propose a selection method that attains the optimal achievable tradeoff (i.e., the optimal ergodic capacity and/or outage probability for any given energy transfer), along with a similar selection method which behaves approximately as the optimal one in certain regions. Nevertheless, as both of these selection methods require global CSI knowledge in each transmission session, the time-sharing and the threshold-checking schemes are of interest in scenarios with limited CSI availability.

Organization: Useful insights regarding the tradeoff between the information transmission to the receiver and the energy transfer to the RF harvester are provided in Section VI, where an extensive discussion on the derived results is given. The tradeoff results pertain to the optimal schemes which are developed in Section V for $N = 2$, as well as the versatile schemes of time-sharing and threshold-checking which apply to any number of relays. These schemes are presented in detail in Section II, and later analyzed in terms of the achievable tradeoff between ergodic capacity and energy transfer (Section III) and the outage performance for a given energy transfer constraint (Section IV). Prior to the analysis, the preliminaries of the considered system model and some fundamental tradeoff features are presented in the ensuing, Section II.

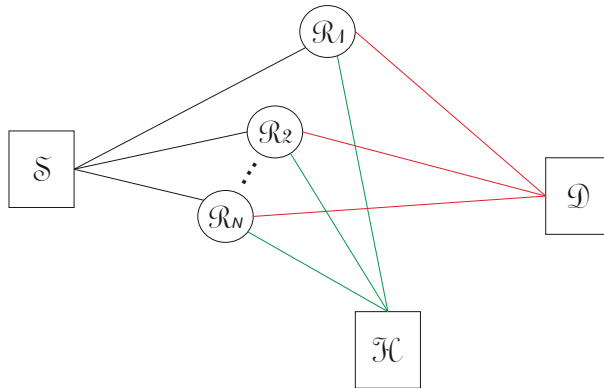


Fig. 1. The considered setup. Red and black lines indicate information transfer; green lines indicate energy transfer.

II. PRELIMINARIES

A. System Model

Sketched in Fig. 1, the considered setup simultaneously transfers information from a source terminal, \mathcal{S} , to a destination terminal, \mathcal{D} , and energy from \mathcal{S} to a harvester terminal, \mathcal{H} . Both the information and energy transferring processes are assisted by a set of half-duplex decode and forward (DF) relays, denoted by \mathcal{R}_i , $i = 1, \dots, N$. All terminals are assumed to be equipped with a single antenna. The information transmission to \mathcal{D} and the energy transfer to \mathcal{H} take place via one of the relays, based on a process described in Subsection II-B.

Let h_{AB} denote the channel between terminals A and B , where $A \in \{\mathcal{S}, \mathcal{R}_1, \dots, \mathcal{R}_N\}$ and $B \in \{\mathcal{R}_1, \dots, \mathcal{R}_N, \mathcal{D}, \mathcal{H}\}$. Let us denote the squared channel gain of the A - B link by $a_{AB} = |h_{AB}|^2$. For simplicity, we assume that the fading in all channels involved is Rayleigh, independent and identically distributed (i.i.d.). However, the analysis can be extended to account for independent but not necessarily identically distributed fading channels as well. The instantaneous signal-to-noise ratio (SNR) of the A - B link is denoted by γ_{AB} , and is exponentially distributed with mean value $\bar{\gamma}$. Moreover, the source and the relay terminals are assumed to transmit with power P .

In DF relaying, the composite \mathcal{S} - \mathcal{R}_i - \mathcal{D} path is dominated by the “bottleneck” link (see e.g. [21]). Hence, the equivalent SNR, γ_i , of the \mathcal{S} - \mathcal{R}_i - \mathcal{D} link, is defined as

$$\gamma_i = \min(\gamma_{\mathcal{S}\mathcal{R}_i}, \gamma_{\mathcal{R}_i\mathcal{D}}). \quad (1)$$

Because $\gamma_{\mathcal{S}\mathcal{R}_i}$ and $\gamma_{\mathcal{R}_i\mathcal{D}}$ are independent exponentially distributed random variables (RVs), γ_i is

also exponentially distributed and its mean value equals half of the mean value of $\gamma_{S\mathcal{R}_i}$ and $\gamma_{\mathcal{R}_i\mathcal{D}}$, i.e.

$$f_{\gamma_i}(x) = \frac{2}{\bar{\gamma}} \exp\left(-\frac{2x}{\bar{\gamma}}\right). \quad (2)$$

We denote by ε_i the energy transferred to \mathcal{H} via the \mathcal{S} - \mathcal{R}_i - \mathcal{H} path, i.e., the harvested energy when \mathcal{R}_i is selected. This energy is given by

$$\varepsilon_i = \beta P a_{\mathcal{R}_i\mathcal{H}} \quad (3)$$

where β , $0 < \beta \leq 1$, denotes the energy absorption coefficient, which equals the energy absorbed by \mathcal{H} when the received power at \mathcal{H} equals one. Roughly speaking, parameter β characterizes the efficiency of the energy harvester [16]. The noise power is assumed identical in all links, and denoted by N_0 . Moreover, we assume that because of large path-loss and/or shadowing no information and energy are transferred via the \mathcal{S} - \mathcal{D} and \mathcal{S} - \mathcal{H} channels, respectively.

B. Relay Selection: General Description

In each transmission frame, a single relay out of the set of available relays is selected. The selected relay is denoted by \mathcal{R}_s : That is, $s = i$ if \mathcal{R}_i is selected, $i = 1, \dots, N$. The selection is assumed to be implemented in a centralized manner. That is, a central unit (CU) collects the CSI of all the links in the system. Based on the collected CSI, the CU decides which relay should be selected for a given transmission frame. Loosely speaking, the decision on the selected relay tries to compromise between the reliability of the information transmission to \mathcal{D} and the total energy transferred to \mathcal{H} .

Let \mathcal{R}_κ denote the relay which maximizes the SNR at \mathcal{D} at a given transmission frame. That is,

$$\kappa = \arg \max_{i=1, \dots, N} \gamma_i. \quad (4)$$

Let \mathcal{R}_λ denote the relay which maximizes the energy transfer to \mathcal{H} at a given transmission frame. That is,

$$\lambda = \arg \max_{i=1, \dots, N} \varepsilon_i. \quad (5)$$

Apparently, as \mathcal{R}_κ and \mathcal{R}_λ are not necessarily identical, the selection of \mathcal{R}_s leads to a tradeoff between information transmission and energy transfer, which is analyzed in detail in Section III. Prior to elaborating on the particular tradeoff of interest, some preliminaries on the tradeoff analysis are in order.

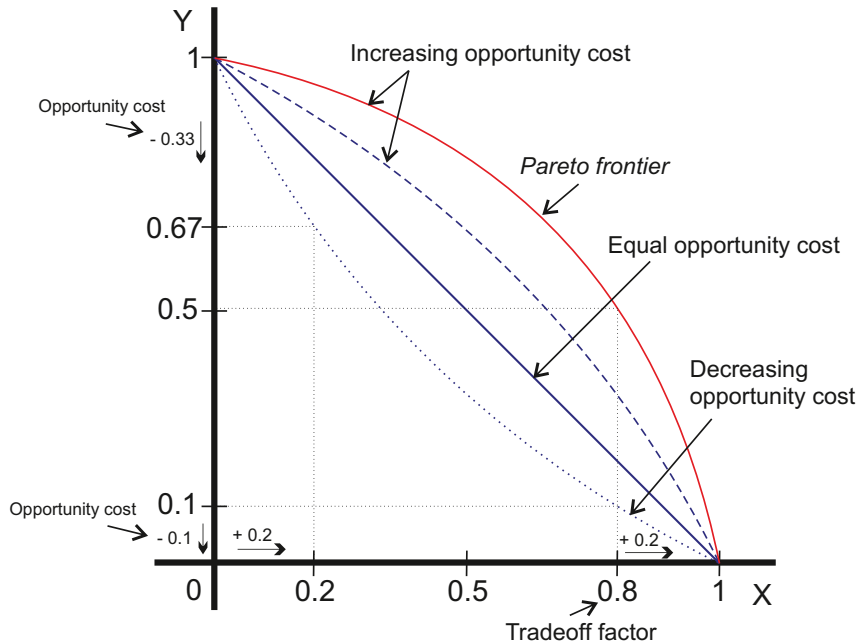


Fig. 2. General tradeoff parameters between two variables, X , Y .

C. Preliminaries of Tradeoff Analysis

In economics and several fields of engineering, a tradeoff is referred to as a situation where one commodity or performance metric, X , is sacrificed in return for gaining another commodity or performance metric, Y [22]. The tradeoff is usually illustrated by a 2-dimensional curve which consists of the set of all feasible (X, Y) pairs. An illustrative example of tradeoff curves is presented in Fig. 2, where the range of the exchanged metrics is normalized to one.

For a better understanding of the subsequent analysis, the following terminology is introduced:

- *Tradeoff factor*: By tradeoff factor, δ ($0 \leq \delta \leq 1$), we refer to the priority of maximizing X over Y . The tradeoff factor specifies the point of operation along the tradeoff curve, i.e., it specifies the quantity of X that is exchanged with Y . When the range of X is normalized to the interval between zero and one (c.f. Fig. 2), the tradeoff factor equals the abscissa of the point of interest.
- *Opportunity cost*: For a given difference of X , the opportunity cost is defined as the corresponding absolute difference of Y [22]. A linear tradeoff curve thus corresponds to an “equal opportunity cost” tradeoff (c.f. Fig. 2, solid blue line), since it entails a constant

exchange between X and Y . A strictly convex tradeoff curve is associated with a tradeoff with “*decreasing opportunity cost*” (c.f. Fig. 2, dotted blue line) while a strictly concave curve corresponds to a tradeoff with “*increasing opportunity cost*” (c.f. Fig. 2, dashed blue line). In practice, tradeoffs with increasing opportunity cost are preferable because they entail a relatively larger gain of one of the two metrics for a given sacrifice of the other.

- *Pareto frontier*: An (X, Y) allocation is considered “Pareto efficient” if there exist no other feasible (X, Y) allocation which results in increasing one metric (X or Y) without decreasing the other [22]. The set of all Pareto efficient points comprises the Pareto frontier (c.f. Fig. 2, red line). The Pareto frontier illustrates the optimal tradeoff between X and Y , in the sense that it provides the largest achievable value of Y (X) given X (Y).

III. TRADEOFF BETWEEN ERGODIC CAPACITY AND AVERAGE TRANSFERRED ENERGY

This section presents an analysis of the tradeoff between the ergodic capacity for information transmission to \mathcal{D} and the average energy transfer to \mathcal{H} . In the sequel, we consider the energy transfer as the reference metric (X) and the ergodic capacity as the cost metric (Y). This tradeoff is governed by the decision regarding the relay selection. That is, since \mathcal{R}_κ and \mathcal{R}_λ do not necessarily coincide with each other, the choice of the activated relay determines how much of the available capacity for information transmission to \mathcal{D} is exchanged for energy transfer to \mathcal{H} , or, in other words, the tradeoff factor. Here, we consider three relay selection schemes, which we dub “time-sharing”, “threshold-checking”, and “weighted difference” schemes, respectively. The three considered schemes have different CSI requirements, thus depending on the CSI availability they can be employed in different application scenarios. The resulting tradeoffs are investigated in Subsections III-B, III-C, and III-D, respectively, while a discussion on their implementation complexity is given in Subsection III-E. Prior to analyzing the specific tradeoffs enabled by the considered schemes, we first study their boundaries, namely the minimum and maximum achievable ergodic capacity and energy transfer. These boundaries are identical for all three schemes.

A. Tradeoff Boundaries

1) Ergodic capacity:

Lemma 1: The minimum and maximum ergodic capacity for information transmission to \mathcal{D} equals, respectively,

$$C_{\min} = \frac{\exp\left(\frac{2}{\bar{\gamma}}\right) \mathcal{E}_1\left(\frac{2}{\bar{\gamma}}\right)}{2 \ln(2)} \quad (6)$$

$$C_{\max} = N \sum_{j=0}^{N-1} \frac{(-1)^j \binom{N-1}{j}}{2(j+1) \ln(2)} \exp\left(2 \frac{j+1}{\bar{\gamma}}\right) \mathcal{E}_1\left(2 \frac{j+1}{\bar{\gamma}}\right) \quad (7)$$

where $\mathcal{E}_n(x) = \int_1^\infty e^{-xy}/(y^n) dy$ is the exponential integral function [23, Eq. (5.1.1)].

Proof: The proof is provided in Appendix A. ■

2) Average Transferred Energy:

Lemma 2: The minimum and maximum average energy transfer to \mathcal{H} equals, respectively,

$$\epsilon_{\min} = \bar{\epsilon} \quad (8)$$

$$\epsilon_{\max} = H_N \bar{\epsilon} \quad (9)$$

where $\bar{\epsilon} = \beta N_0 \bar{\gamma}$ is the expectation of ϵ_i and H_N denotes the harmonic number of N defined as $H_N = \sum_{i=1}^N (1/i)$.

Proof: Since the maximum energy transfer occurs for $s = \lambda$, (9) is obtained as the first order moment of N i.i.d. exponentially distributed RVs [24]. Eq. (8) is trivially obtained by assuming that the relay selection process is independent of $a_{\mathcal{R}_i \mathcal{H}}$, $i = 1, \dots, N$. ■

3) *Tradeoff factor:* Let ϵ denote the average (long-term) energy harvested by \mathcal{H} . Out of the two exchanged metrics (i.e., capacity C and energy transfer ϵ), ϵ is considered as the reference metric. Hence, the tradeoff factor, δ ($0 \leq \delta \leq 1$), is the percentage of the range of possible energy transfer that is actually transferred to \mathcal{H} . Considering the boundaries of ϵ given in (9), (8), we can express ϵ in terms of the tradeoff factor as $\epsilon = [1 + \delta(H_N - 1)] \bar{\epsilon}$. The tradeoff factor is thus obtained by solving this expression with respect to δ , yielding

$$\delta = \frac{\frac{\epsilon}{\bar{\epsilon}} - 1}{H_N - 1}. \quad (10)$$

B. Time-Sharing Selection Scheme

The time-sharing scheme is considered as a simplistic selection method which operates as follows: In each transmission frame, the CU selects either \mathcal{R}_κ or \mathcal{R}_λ in a pseudorandom fashion. That is,

\mathcal{R}_κ is selected with probability μ ; \mathcal{R}_λ is selected with probability $1 - \mu$, i.e.

$$s = \begin{cases} \kappa, & \text{with probability } \mu \\ \lambda, & \text{with probability } 1 - \mu \end{cases}. \quad (11)$$

This strategy ensures that, in the long run, the percentage of transmission frames allocated for optimum information transmission and optimum energy transfer is controllable.

The capacity of the time-sharing scheme equals C_{\max} for the time frames when $s = \kappa$, and C_{\min} for the time frames where $s = \lambda$. Consequently, the ergodic capacity is obtained as

$$C_{TS} = \mu C_{\max} + (1 - \mu) C_{\min}. \quad (12)$$

Similarly, the energy transfer to \mathcal{H} equals ϵ_{\min} if $s = \kappa$ and ϵ_{\max} if $s = \lambda$. Hence, the average energy transferred to \mathcal{H} when the time-sharing selection method is employed is given by

$$\epsilon_{TS} = \mu \bar{\epsilon} + (1 - \mu) \bar{\epsilon} H_N = \bar{\epsilon} [\mu + (1 - \mu) H_N]. \quad (13)$$

Solving (13) with respect to μ yields

$$\mu = \frac{\bar{\epsilon} H_N - \epsilon_{TS}}{\bar{\epsilon} (H_N - 1)}. \quad (14)$$

By plugging (14) into (12), C_{TS} is expressed as a function of ϵ_{TS} as follows

$$C_{TS} = \frac{e^{\frac{2}{\gamma}} (\epsilon_{TS} - \bar{\epsilon}) \mathcal{E}_1\left(\frac{2}{\gamma}\right) + (\bar{\epsilon} H_N - \epsilon_{TS}) \ln(4) \sum_{j=0}^{N-1} \frac{N(-1)^j e^{\frac{2(j+1)}{\gamma}} \binom{N-1}{j} \mathcal{E}_1\left(\frac{2(j+1)}{\gamma}\right)}{2^{(j+1)} \ln(2)}}{2\bar{\epsilon} (H_N - 1) \ln(2)}. \quad (15)$$

Corollary 1: The time-sharing scheme results in an equal opportunity cost between ergodic capacity and average energy transfer.

Proof: The proof follows directly from (15), by noting that C_{TS} is a linear function of ϵ_{TS} . ■

C. Threshold-Checking Selection Scheme

The time-sharing scheme gives insight into the tradeoff between information transmission and energy transfer, yet, clearly, it is far from making full use of the relays. Thus, we consider an alternative selection scheme, which operates as follows. In each transmission session the SNR of the $\mathcal{S}\text{-}\mathcal{R}_\kappa\text{-}\mathcal{D}$ link, γ_κ , is compared to a threshold, τ . If $\gamma_\kappa \geq \tau$, then \mathcal{R}_κ is activated. Otherwise, \mathcal{R}_λ is activated. In mathematical terms,

$$s = \begin{cases} \kappa, & \text{if } \gamma_\kappa \geq \tau \\ \lambda, & \text{if } \gamma_\kappa < \tau \end{cases}. \quad (16)$$

Naturally, this selection scheme is expected to lead to a better capacity-energy transfer tradeoff. A rigorous analysis of this tradeoff follows.

Considering the threshold-checking scheme's mode of operation, the ergodic capacity of the information transfer to \mathcal{D} is obtained as (for the derivation, please refer to Appendix B)

$$\begin{aligned}
C_{TC} &= E \{C_\kappa | \gamma_\kappa \geq \tau\} \Pr \{\gamma_\kappa \geq \tau\} + E \{C_\lambda | \gamma_\kappa < \tau\} \Pr \{\gamma_\kappa < \tau\} \\
&= \sum_{j=0}^{M-1} \frac{N (-1)^j \binom{N-1}{j} e^{-\frac{2(j+1)\tau}{\bar{\gamma}}} \left[e^{\frac{2(j+1)(\tau+1)}{\bar{\gamma}}} \mathcal{E}_1 \left(\frac{2(j+1)(\tau+1)}{\bar{\gamma}} \right) + \ln(\tau+1) \right]}{2(j+1) \ln(2)} \\
&\quad + \frac{e^{\frac{2}{\bar{\gamma}}} \left[\mathcal{E}_1 \left(\frac{2}{\bar{\gamma}} \right) - \mathcal{E}_1 \left(\frac{2(1+\tau)}{\bar{\gamma}} \right) \right] - e^{-\frac{2\tau}{\bar{\gamma}}} \ln(1+\tau)}{2 \ln(2)} \left(1 - e^{-\frac{2\tau}{\bar{\gamma}}} \right)^{N-1}
\end{aligned} \tag{17}$$

where $E \{\cdot\}$ denotes expectation. Similarly to (13), the average energy transfer to \mathcal{H} is obtained as

$$\begin{aligned}
\epsilon_{TC} &= \Pr \{\gamma_\kappa \geq \tau\} \bar{\epsilon} + \Pr \{\gamma_\kappa < \tau\} \int_0^\infty x f_{\epsilon_\lambda}(x) dx \\
&= \left[1 - \left(1 - e^{-\frac{2\tau}{\bar{\gamma}}} \right)^N \right] \bar{\epsilon} + \left(1 - e^{-\frac{2\tau}{\bar{\gamma}}} \right)^N \bar{\epsilon} H_N.
\end{aligned} \tag{18}$$

Solving (18) with respect to τ yields

$$\tau = \bar{\gamma} \ln \left[\left(1 - \sqrt[N]{\frac{\epsilon_{TC} - \bar{\epsilon}}{\bar{\epsilon}(H_N - 1)}} \right)^{-1/2} \right]. \tag{19}$$

Substituting (19) into (17), we can express C_{TC} as a function of ϵ_{TC} , as shown below

$$\begin{aligned}
C_{TC} &= \frac{\left(\frac{\epsilon_{TC} - \bar{\epsilon}}{\bar{\epsilon}(H_N - 1)} \right)^{\frac{N-1}{N}}}{2 \ln(2)} \left[e^{\frac{2}{\bar{\gamma}}} \mathcal{E}_1 \left(\frac{2}{\bar{\gamma}} \right) - e^{\frac{2}{\bar{\gamma}}} \mathcal{E}_1 \left(\frac{2}{\bar{\gamma}} - \ln \left(1 - \sqrt[N]{\frac{\epsilon_{TC} - \bar{\epsilon}}{\bar{\epsilon}(H_N - 1)}} \right) \right) \right] \\
&\quad - \left(1 - \sqrt[N]{\frac{\epsilon_{TC} - \bar{\epsilon}}{\bar{\epsilon}(H_N - 1)}} \right) \ln \left(1 - \frac{\bar{\gamma} \ln \left(1 - \sqrt[N]{\frac{\epsilon_{TC} - \bar{\epsilon}}{\bar{\epsilon}(H_N - 1)}} \right)}{2} \right) \\
&\quad + \frac{e^{\frac{2(j+1)}{\bar{\gamma}} \left[1 - \frac{\bar{\gamma}}{2} \ln \left(1 - \sqrt[N]{\frac{\epsilon_{TC} - \bar{\epsilon}}{\bar{\epsilon}(H_N - 1)}} \right) \right]} \mathcal{E}_1 \left(\frac{2(j+1) \left[1 - \frac{\bar{\gamma}}{2} \ln \left(1 - \sqrt[N]{\frac{\epsilon_{TC} - \bar{\epsilon}}{\bar{\epsilon}(H_N - 1)}} \right) \right]}{\bar{\gamma}} \right) + \ln \left[1 - \frac{\bar{\gamma}}{2} \ln \left(1 - \sqrt[N]{\frac{\epsilon_{TC} - \bar{\epsilon}}{\bar{\epsilon}(H_N - 1)}} \right) \right]}{2 \left[N \binom{N-1}{j} \left[1 - \sqrt[N]{\frac{\epsilon_{TC} - \bar{\epsilon}}{\bar{\epsilon}(H_N - 1)}} \right]^{j+1} \right]^{-1} (-1)^j (j+1) \ln(2)}.
\end{aligned} \tag{20}$$

Corollary 2: The tradeoff between ergodic capacity and average energy transfer of the threshold-checking scheme is an increasing opportunity cost tradeoff.

Proof: The proof follows by showing that $\partial^2 C_{TC} / \partial \epsilon_{TC}^2 < 0$ for each $\bar{\epsilon} < \epsilon_{TC} < H_N \bar{\epsilon}$. \blacksquare

D. Weighted Difference Selection Scheme

Let us now focus on the case of $N = 2$, i.e., the case where two relays are available. For this case, the weighted difference selection method operates as follows

$$\gamma_1 - \gamma_2 \underset{s=2}{\overset{s=1}{>}} \nu (\varepsilon_2 - \varepsilon_1) \quad (21)$$

where $\nu > 0$ is a constant characterizing the tradeoff factor.

1) *Intuition Behind the Weighted Difference Scheme:* The intuition behind the weighted difference selection policy in (21) is simple: If one of the two relays experiences stronger links to \mathcal{D} and \mathcal{H} than the other, then this relay should be selected. Otherwise, the relay with stronger channel to \mathcal{D} is selected if more priority is given to information transmission than to energy transfer, and vice versa. This intuition is clearly illustrated in (21): If \mathcal{R}_1 , for instance, is superior (inferior) to \mathcal{R}_2 in terms of both information and energy transfer, then the left hand side of (21) will be positive (negative) and the right hand side of (21) negative (positive), leading to $s = 1$ ($s = 2$). If, on the other hand, \mathcal{R}_1 is superior (inferior) to \mathcal{R}_2 in terms of information rate but inferior (superior) to \mathcal{R}_2 in terms of energy transfer, then the two sides of (21) have the same sign hence the selected relay is determined by the weighting coefficient, ν . Clearly, ν can take any positive real value therefore any desired tradeoff factor can be achieved by properly adjusting ν .

2) *Tradeoff Expression:* An expression for the tradeoff achieved by the weighted difference scheme is provided in the ensuing Proposition.

Proposition 1: The capacity-energy tradeoff of the weighted difference scheme is given by

$$C_{WD} = \frac{2 \left[1 - \left(1 - \sqrt{\frac{\bar{\varepsilon}}{3\bar{\varepsilon} - 2\epsilon_{WD}}} \right)^2 \right] \mathcal{E}_1 \left(\frac{2}{\bar{\gamma}} \right) - e^{\frac{2}{\bar{\gamma}}} \mathcal{E}_1 \left(\frac{4}{\bar{\gamma}} \right)}{2e^{-\frac{2}{\bar{\gamma}}} \left[1 - \left(1 - \sqrt{\frac{\bar{\varepsilon}}{3\bar{\varepsilon} - 2\epsilon_{WD}}} \right)^2 \right] \ln(2)} + \frac{\exp \left(-\frac{2}{\bar{\gamma} \left(1 - \sqrt{\frac{\bar{\varepsilon}}{3\bar{\varepsilon} - 2\epsilon_{WD}}} \right)} \right) \left(1 - \sqrt{\frac{\bar{\varepsilon}}{3\bar{\varepsilon} - 2\epsilon_{WD}}} \right)^2 \mathcal{E}_1 \left(\frac{2 \left(\frac{1}{1 - \sqrt{\frac{\bar{\varepsilon}}{3\bar{\varepsilon} - 2\epsilon_{WD}}} - 1} \right)}{\bar{\gamma}} \right)}{2e^{-\frac{2}{\bar{\gamma}}} \left[1 - \left(1 - \sqrt{\frac{\bar{\varepsilon}}{3\bar{\varepsilon} - 2\epsilon_{WD}}} \right)^2 \right] \ln(2)}. \quad (22)$$

Proof: The proof is provided in Appendix C. ■

Corollary 3: The tradeoff between ergodic capacity and average energy transfer of the weighted difference scheme is an increasing opportunity cost tradeoff.

TABLE I
CSI REQUIREMENTS AND APPLICATION SCENARIOS OF THE THREE CONSIDERED SCHEMES

Relay Selection Scheme	CSI Requirements	Number of Relays
<i>Time-Sharing Scheme</i>	Low	$N \geq 2$
<i>Threshold-Checking Scheme</i>	Medium	$N \geq 2$
<i>Weighted Difference Scheme</i>	High	$N = 2$

Proof: Similarly to Corollary 2, the proof follows by taking the second derivative of C_{WD} with respect to ϵ_{WD} and noting that $\partial^2 C_{WD} / \partial \epsilon_{WD}^2 < 0$ for each $\bar{\epsilon} < \epsilon_{WD} < H_N \bar{\epsilon}$. ■

As shown later in Section VI, the weighted difference scheme leads to a capacity-energy tradeoff that is close to the Pareto frontier. However, it applies only for $N = 2$. An extension to $N > 2$ is not straightforward since in that case multiple comparisons among the candidate relays in terms of their contributions to the overall capacity and the overall energy transfer would be required.

E. On the CSI Requirements of the Proposed Schemes

Here, we provide a brief discussion on the implementation complexity of the three schemes under consideration, in terms of the amount of CSI required for their operation. The time-sharing scheme has the lowest CSI requirement of the three, because it requires CSI knowledge of either the S - \mathcal{R} - \mathcal{D} or the \mathcal{R} - \mathcal{H} links. The threshold-checking scheme requires continuous CSI knowledge of the S - \mathcal{R} - \mathcal{D} links; it additionally requires CSI knowledge of the \mathcal{R} - \mathcal{H} links for as long as the strength of the end-to-end channel to \mathcal{D} is below a given threshold. The weighted difference scheme requires continuous CSI knowledge for all S - \mathcal{R} - \mathcal{D} and \mathcal{R} - \mathcal{H} links. Consequently, the time-sharing scheme has relatively low, the threshold-checking scheme medium, and the weighted difference scheme high requirements regarding CSI knowledge. For the reader's convenience, the CSI requirements of the proposed schemes are summarized in Table I.

IV. OUTAGE AND ASYMPTOTIC PERFORMANCE FOR A GIVEN ENERGY TRANSFER

A. Outage Probability

For schemes with constant transmission rate where the source does not have transmit-side CSI, an outage occurs if the end-to-end link to the destination cannot support the transmission rate. In DF relaying, an outage in the $\mathcal{S}\text{-}\mathcal{R}_i\text{-}\mathcal{D}$ link occurs if either the $\mathcal{S}\text{-}\mathcal{R}_i$ or the $\mathcal{R}_i\text{-}\mathcal{D}$ link is in outage. Consequently, denoting the fixed transmission rate by r , an outage occurs if the end-to-end SNR of the active relay, γ_s , drops below the threshold $\gamma_{\text{th}} = 2^{2r} - 1$. Here, we provide expressions for the outage probability of the three considered schemes, assuming that a prescribed amount of energy is transferred to \mathcal{H} .

1) *Outage Probability of the Time-Sharing Scheme:* The simplicity of the mode of operation of the time-sharing scheme shown in (11) allows for a straightforward evaluation of the outage probability as

$$\begin{aligned} P_{out,TS} &= \mu \Pr \{ \gamma_{\kappa} < \gamma_{\text{th}} \} + (1 - \mu) \Pr \{ \gamma_{\lambda} < \gamma_{\text{th}} \} \\ &= \mu \left(1 - e^{-\frac{2\gamma_{\text{th}}}{\bar{\gamma}}} \right)^N + (1 - \mu) \left(1 - e^{-\frac{2\gamma_{\text{th}}}{\bar{\gamma}}} \right). \end{aligned} \quad (23)$$

Substituting μ from (14) into (23) yields the outage probability of the time-sharing scheme as a function of ϵ_{TS} and $\bar{\epsilon}$,

$$P_{out,TS} = \frac{e^{-\frac{2\gamma_{\text{th}}}{\bar{\gamma}}} \left\{ 1 - \frac{\epsilon_{TS}}{\bar{\epsilon}} + e^{\frac{2\gamma_{\text{th}}}{\bar{\gamma}}} \left[\frac{\epsilon_{TS}}{\bar{\epsilon}} + \left(H_N - \frac{\epsilon_{TS}}{\bar{\epsilon}} \right) \left(1 - e^{-\frac{2\gamma_{\text{th}}}{\bar{\gamma}}} \right)^N - 1 \right] \right\}}{H_N - 1}. \quad (24)$$

Alternatively, using (10) we can express the outage probability as a function of the tradeoff factor, δ , as

$$P_{out,TS} = (1 - \delta) \left(1 - e^{-\frac{2\gamma_{\text{th}}}{\bar{\gamma}}} \right)^N + \delta \left(1 - e^{-\frac{2\gamma_{\text{th}}}{\bar{\gamma}}} \right). \quad (25)$$

In fact, the expression in (25) was expected since it is clear from (11) that for the time-sharing scheme, $\delta = 1 - \mu$.

2) *Outage Probability of the Threshold-Checking Scheme:* Considering the relay selection policy in the threshold-checking scheme in (16), for calculating the outage probability we consider the following cases:

- If $\tau \leq \gamma_{\text{th}}$, then the outage performance is determined by γ_{κ} , hence an outage occurs if $\gamma_{\kappa} < \gamma_{\text{th}}$.

- If $\tau > \gamma_{\text{th}}$, then an outage occurs if $\gamma_\lambda < \gamma_{\text{th}}$. The outage event in this case is thus equivalent to the event where the SNR of a randomly selected relay – out of the pool of N relays – is smaller than γ_{th} , while the SNRs of the remaining $N - 1$ relays are all smaller than τ .

The overall outage probability is thus expressed as

$$P_{out,TC} = \begin{cases} \left(1 - e^{-\frac{2\gamma_{\text{th}}}{\bar{\gamma}}}\right)^N, & \text{if } \tau \leq \gamma_{\text{th}} \\ \left(1 - e^{-\frac{2\gamma_{\text{th}}}{\bar{\gamma}}}\right) \left(1 - e^{-\frac{2\tau}{\bar{\gamma}}}\right)^{N-1}, & \text{if } \tau > \gamma_{\text{th}} \end{cases}. \quad (26)$$

By replacing τ in (26) with the right-hand side of (19) we can express the outage probability of the threshold-checking scheme as a function of ϵ_{TC} and $\bar{\epsilon}$,

$$P_{out,TC} = \begin{cases} \left(1 - e^{-\frac{2\gamma_{\text{th}}}{\bar{\gamma}}}\right)^N, & \text{if } \frac{\epsilon_{TC}}{\bar{\epsilon}} \leq 1 + (H_N - 1) \left(1 - e^{-\frac{2\gamma_{\text{th}}}{\bar{\gamma}}}\right)^N \\ \left(1 - e^{-\frac{2\gamma_{\text{th}}}{\bar{\gamma}}}\right) \left(\frac{\epsilon_{TC} - 1}{H_N - 1}\right)^{N-1}, & \text{if } \frac{\epsilon_{TC}}{\bar{\epsilon}} > 1 + (H_N - 1) \left(1 - e^{-\frac{2\gamma_{\text{th}}}{\bar{\gamma}}}\right)^N \end{cases}. \quad (27)$$

Alternatively, $P_{out,TC}$ is expressed as a function of the tradeoff factor as

$$P_{out,TC} = \begin{cases} \left(1 - e^{-\frac{2\gamma_{\text{th}}}{\bar{\gamma}}}\right)^N, & \text{if } \delta \leq \left(1 - e^{-\frac{2\gamma_{\text{th}}}{\bar{\gamma}}}\right)^N \\ \left(1 - e^{-\frac{2\gamma_{\text{th}}}{\bar{\gamma}}}\right) \delta^{\frac{N-1}{N}}, & \text{if } \delta > \left(1 - e^{-\frac{2\gamma_{\text{th}}}{\bar{\gamma}}}\right)^N \end{cases}. \quad (28)$$

3) Outage Probability of the Weighted Difference Scheme:

Proposition 2: The outage probability of the weighted difference scheme is given by

$$P_{out,WD} = \frac{e^{-\frac{4\gamma_{\text{th}}}{\bar{\gamma}}} \left(e^{\frac{2\gamma_{\text{th}}}{\bar{\gamma}}} - 1\right)^2 + \left(1 - \sqrt{\frac{\bar{\epsilon}}{3\bar{\epsilon} - 2\epsilon_{WD}}}\right)^2 \left[e^{\frac{2\gamma_{\text{th}}}{\bar{\gamma}}} \left(2 - e^{\frac{2\gamma_{\text{th}}}{\bar{\gamma}} \left(1 - \sqrt{\frac{\bar{\epsilon}}{3\bar{\epsilon} - 2\epsilon_{WD}}}\right)}\right) - 1 \right]}{1 - \left(1 - \sqrt{\frac{\bar{\epsilon}}{3\bar{\epsilon} - 2\epsilon_{WD}}}\right)^2} \quad (29)$$

or, in terms of the tradeoff factor, as

$$P_{out,WD} = \frac{e^{-\frac{4\gamma_{\text{th}}}{\bar{\gamma}}} \left(e^{\frac{2\gamma_{\text{th}}}{\bar{\gamma}}} - 1\right)^2 + \left(1 - \sqrt{\frac{1}{1-\delta}}\right)^2 \left[e^{\frac{2\gamma_{\text{th}}}{\bar{\gamma}}} \left(2 - e^{\frac{2\gamma_{\text{th}}}{\bar{\gamma}} \left(1 - \sqrt{\frac{1}{1-\delta}}\right)}\right) - 1 \right]}{1 - \left(1 - \sqrt{\frac{1}{1-\delta}}\right)^2}. \quad (30)$$

Proof: The proof is provided in Appendix D. ■

B. Asymptotic Analysis

By taking the Taylor series expansion and keeping only the first order terms, (25), (28), and (30) reduce after some algebraic manipulations to the following high-SNR expressions

$$P_{out,TS} \approx \frac{2\gamma_{\text{th}}}{\bar{\gamma}} \delta \quad (31)$$

$$P_{out,TC} \approx \frac{2\gamma_{th}}{\bar{\gamma}} \delta^{\frac{N-1}{N}} \quad (32)$$

$$P_{out,WD} \approx \frac{2\gamma_{th}}{\bar{\gamma}} \left(1 - \sqrt{1 - \delta}\right). \quad (33)$$

Using the fact that $1 - \sqrt{1 - \delta} < \delta < \sqrt{\delta}$ for $0 < \delta < 1$, we observe from (31)-(33) that for $N = 2$ and for any tradeoff factor the best asymptotic outage performance is achieved by the weighted difference scheme, the time-sharing scheme performs in the middle of the other two, and the worst asymptotic outage performance is achieved by the threshold-checking scheme. The same result holds also for $N > 2$, as $\delta < \delta^{\frac{N-1}{N}}$ for any $0 < \delta < 1$. As will be shown via numerical examples in Section VI, the outcome of this comparison is different from that in terms of the ergodic capacity, as for the latter comparison the threshold-checking scheme outperforms the time-sharing scheme.

Using (31)-(33), the diversity gain, \mathcal{G}_d , and array gain, \mathcal{G}_a , can be straightforwardly derived by expressing the asymptotic outage probability in the form $P_{out} = (\mathcal{G}_a \bar{\gamma} / \gamma_{th})^{-\mathcal{G}_d}$ [25]. The results are summarized in the ensuing two Corollaries.

Corollary 4: The diversity order of the time-sharing, threshold-checking, and weighted difference schemes equals one, unless a zero tradeoff factor is employed. In other words, if the required energy transfer to \mathcal{H} pertaining to the above mentioned selection schemes is larger (even by an infinitesimally small amount) than its lower boundary, ϵ_{\min} , then the diversity gain is lost.

Corollary 5: The array gain of the time-sharing, threshold-checking and weighted difference scheme equal respectively

$$\mathcal{G}_{a,TS} = \frac{1}{2\delta} \quad (34)$$

$$\mathcal{G}_{a,TC} = \frac{1}{2\delta^{\frac{N-1}{N}}} \quad (35)$$

$$\mathcal{G}_{a,WD} = \frac{1}{2(1 - \sqrt{1 - \delta})}. \quad (36)$$

V. PARETO EFFICIENCY FOR $N = 2$

The idea behind the weighted difference scheme is general enough so that by a careful amendment of the quantities in the left hand side of (21), we can choose to optimize any long-term performance metric associated with information transmission to \mathcal{D} , for a given energy transfer to \mathcal{H} and $N = 2$. This interesting conclusion is summarized in the ensuing Theorem.

Theorem 1: Let \mathcal{F} denote any metric that characterizes the long-term performance of the information transmission to \mathcal{D} , in the sense that the performance is optimized when \mathcal{F} is maximized.

Let $\mathcal{F}(\gamma_i)$ be a non-decreasing function of γ_i , which describes the instantaneous realization of \mathcal{F} associated with the use of the $\mathcal{S}\text{-}\mathcal{R}_i\text{-}\mathcal{D}$ link. The Pareto frontier of the tradeoff between \mathcal{F} and the average energy transfer is achieved by the following selection policy

$$\mathcal{F}(\gamma_1) - \mathcal{F}(\gamma_2) \underset{s=2}{\overset{s=1}{>}} \zeta (\varepsilon_2 - \varepsilon_1) \quad (37)$$

where $\zeta > 0$ is a constant, in which the tradeoff factor is reflected.

Proof: The proof is provided in Appendix E. ■

The utility parameter \mathcal{F} in (37) can represent any of the most common performance metrics whose maximization is associated with optimizing system performance, such as the average SNR, the ergodic capacity, the probability of no-outage, and the probability of correct bit detection. If the average SNR is the metric of interest, then the weighted difference scheme is Pareto efficient because (37) reduces to (21). Next, we investigate the tradeoffs pertaining to the optimal ergodic capacity and the optimal probability of no-outage for a given energy transfer. The analysis for the optimal probability of correct bit detection follows similarly, and is omitted here for brevity.

A. Optimal Ergodic Capacity for a Given Energy Transfer

Theorem 1 provides the Pareto frontier of the tradeoff between ergodic capacity and average transferred energy by substituting $\mathcal{F}(\gamma_i)$ with the instantaneous capacity expression, i.e., by setting

$$\mathcal{F}(\gamma_1) = \frac{1}{2} \log_2(1 + \gamma_1), \quad \mathcal{F}(\gamma_2) = \frac{1}{2} \log_2(1 + \gamma_2) \quad (38)$$

in (37).

The Pareto Frontier of Ergodic Capacity Vs. Energy Transfer: Due to the complicated mathematical analysis involved, the exact derivation of the Pareto frontier of the desired tradeoff is cumbersome. In fact, by following a similar approach as that in Appendix C (the parameters $(\gamma_2 - \gamma_1)/\nu$ and $(\gamma_1 - \gamma_2)/\nu$ at the integral limits of the fourth integral in \mathcal{I}_{2a} , \mathcal{I}_{2b} , \mathcal{I}_{3a} , \mathcal{I}_{3b} in (49) are substituted by $\frac{1}{2\zeta} \log_2(1 + \gamma_2) - \frac{1}{2\zeta} \log_2(1 + \gamma_1)$ and $\frac{1}{2\zeta} \log_2(1 + \gamma_1) - \frac{1}{2\zeta} \log_2(1 + \gamma_2)$, respectively), we can express ε as a function of ζ , yet that expression involves a two-fold integration which, to the best of our knowledge, is solvable only by numerical methods. Thus, the resulting Pareto frontier curve can be derived numerically only. Further discussions on this Pareto frontier are provided in Section VI.

B. Optimal Outage Probability for a Given Energy Transfer

In case the outage probability is the metric of interest, then $\mathcal{F}(\gamma_i)$ in (37) is substituted by

$$\mathcal{F}(\gamma_1) = \begin{cases} 1, & \text{if } \gamma_1 > \gamma_{\text{th}} \\ 0, & \text{if } \gamma_1 < \gamma_{\text{th}} \end{cases}, \quad \mathcal{F}(\gamma_2) = \begin{cases} 1, & \text{if } \gamma_2 > \gamma_{\text{th}} \\ 0, & \text{if } \gamma_2 < \gamma_{\text{th}} \end{cases}. \quad (39)$$

That is, for optimizing the outage probability for a given energy transfer the function $\mathcal{F}(\gamma_i)$ in (37) reduces to the binary event of no-outage, given the instantaneous realization of γ_i , $i = 1, 2$. The resulting tradeoff between the probability of no-outage and the average energy transfer is Pareto efficient, and is investigated below.

The Pareto Frontier of Probability of No-Outage Vs. Energy Transfer: By following a similar analysis as that in Appendix D, the average transferred energy, $\epsilon_{out,opt}$, can be expressed as

$$\begin{aligned} \epsilon_{out,opt} &= \underbrace{\frac{3}{2}e^{-\frac{4\gamma_{\text{th}}}{\bar{\zeta}}}\bar{\epsilon}}_{\text{Case of } \gamma_1 > \gamma_{\text{th}}; \gamma_2 > \gamma_{\text{th}}} + 2 \underbrace{\frac{e^{-\frac{4\gamma_{\text{th}}}{\bar{\zeta}} - \frac{1}{\zeta\bar{\epsilon}}}\left(e^{\frac{2\gamma_{\text{th}}}{\bar{\zeta}}}-1\right)\left[\zeta\bar{\epsilon}\left(2e^{\frac{1}{\zeta\bar{\epsilon}}}+1\right)+1\right]}{2\zeta}}_{\text{Cases of } \gamma_1 < \gamma_{\text{th}}; \gamma_2 > \gamma_{\text{th}}, \gamma_1 > \gamma_{\text{th}}; \gamma_2 < \gamma_{\text{th}}} + \underbrace{\frac{3}{2}\left(1-e^{-\frac{4\gamma_{\text{th}}}{\bar{\zeta}}}\right)^2\bar{\epsilon}}_{\text{Case of } \gamma_1 < \gamma_{\text{th}}; \gamma_2 < \gamma_{\text{th}}} \\ &= \frac{e^{-\frac{4\gamma_{\text{th}}}{\bar{\zeta}}}}{2} \left[\bar{\epsilon} \left(2 - 2e^{\frac{2\gamma_{\text{th}}}{\bar{\zeta}}} + 3e^{\frac{4\gamma_{\text{th}}}{\bar{\zeta}}} \right) + \frac{2e^{-\frac{1}{\zeta\bar{\epsilon}}}(\zeta\bar{\epsilon}+1)\left(e^{\frac{2\gamma_{\text{th}}}{\bar{\zeta}}}-1\right)}{\zeta} \right]. \end{aligned} \quad (40)$$

An important observation that is made from (40) is that the lower boundary of the average transferred energy in this case is different from the lower boundary shown in Lemma 2. In particular, by taking limits in (40) for $\zeta \rightarrow 0^+$, we obtain¹

$$\epsilon_{out,opt,min} = \bar{\epsilon} \left(\frac{3}{2} + e^{-\frac{4\gamma_{\text{th}}}{\bar{\zeta}}} - e^{-\frac{2\gamma_{\text{th}}}{\bar{\zeta}}} \right). \quad (41)$$

This result reveals that the selection policy in (37) (in conjunction with (39)) achieves the Pareto frontier for a limited range of tradeoff factor. In particular, it follows from (10) and (41) that the tradeoff factor in this case spans the interval

$$\delta \in \left[1 - 2 \left(e^{-\frac{2\gamma_{\text{th}}}{\bar{\zeta}}} - e^{-\frac{4\gamma_{\text{th}}}{\bar{\zeta}}} \right), 1 \right]. \quad (42)$$

The limited range of the tradeoff factor can be explained by the fact that a tradeoff in this case exists only for $\mathcal{F}(\gamma_1) \neq \mathcal{F}(\gamma_2)$, since for the complementary event of $\mathcal{F}(\gamma_1) = \mathcal{F}(\gamma_2)$ the left-hand side

¹In fact, $\epsilon_{out,opt,min}$ experiences a discontinuity for $\zeta = 0$, as for this case it is clear from (37) that the scheme reduces to ignoring the energy transfer when selecting the relay, resulting in $\epsilon_{out,opt,min} = \bar{\epsilon}$. This case, however, is excluded from our analysis as it does not result in any tradeoff between probability of no-outage and energy transfer.

of (37) equals zero, hence the relay selection policy is independent of ζ . In other words, no exchange takes place between outage probability and energy transfer as long as $\mathcal{F}(\gamma_1) = \mathcal{F}(\gamma_2)$, an event which occurs with probability $1 - 2 \left(e^{-\frac{2\gamma_{\text{th}}}{\bar{\gamma}}} - e^{-\frac{4\gamma_{\text{th}}}{\bar{\gamma}}} \right)$. The practical meaning of this observation is that the selection policy in (37), (39), achieves an energy transfer increase from $\bar{\epsilon}$ to $\epsilon_{out,opt,min}$ with no outage cost. This fact will be better explained through numerical examples in Section VI-B.

Since (40) is not solvable with respect to ζ , a mathematical expression for the Pareto probability of no-outage as a function of the average energy transfer is not possible. Hence, we confine ourselves to obtaining an expression for the probability of no-outage as a function of ζ , as follows. The no-outage event occurs for the following cases: $\gamma_1 > \gamma_{\text{th}}$ and $\gamma_2 > \gamma_{\text{th}}$; $\gamma_1 > \gamma_{\text{th}}$ and $\gamma_2 < \gamma_{\text{th}}$ and $\epsilon_2 < \epsilon_1 + 1/\zeta$; $\gamma_1 < \gamma_{\text{th}}$ and $\gamma_2 > \gamma_{\text{th}}$ and $\epsilon_1 < \epsilon_2 + 1/\zeta$. The probability of the union of these events can be evaluated by solving the corresponding integrals, which are similar to the integrals in (49), yielding

$$P_{no-out,opt} = e^{-\frac{4\gamma_{\text{th}}}{\bar{\gamma}}} \left[2e^{\frac{2\gamma_{\text{th}}}{\bar{\gamma}}} - e^{-\frac{1}{\zeta\bar{\epsilon}}} \left(e^{\frac{2\gamma_{\text{th}}}{\bar{\gamma}}} - 1 \right) - 1 \right]. \quad (43)$$

VI. NUMERICAL EXAMPLES

This section presents a set of illustrative examples that provide insight into the behavior of the ergodic capacity and the outage probability, for a given required average energy transfer to \mathcal{H} .

A. Ergodic Capacity vs. Energy Transfer

Fig. 3 depicts the ergodic capacity vs. the average energy transferred to \mathcal{H} (normalized with respect to $\bar{\epsilon}$), for the case of two available relays $N = 2$ and $\bar{\gamma} = 20$ dB. The performance of the three tradeoff schemes studied in Section III is compared with the Pareto frontier developed in Section V, for the range of feasible transmitted energy values, i.e., for $\bar{\epsilon} < \epsilon < H_2\bar{\epsilon} = 1.5\bar{\epsilon}$. The curves pertaining to the three schemes in Section III were obtained from (15), (20), and (22). For the generation of the Pareto frontier curve numerical methods were used for obtaining the value of ζ that leads to certain average energy transfer, as described in Section V-A; this value of ζ was then used for obtaining numerical values for the corresponding ergodic capacity. As expected, the time-sharing scheme leads to a linear tradeoff curve (equal opportunity cost) which lies below the tradeoff curves of the threshold-checking and weighted difference scheme, since the two latter schemes achieve tradeoffs with increasing opportunity costs. Moreover, it is observed that

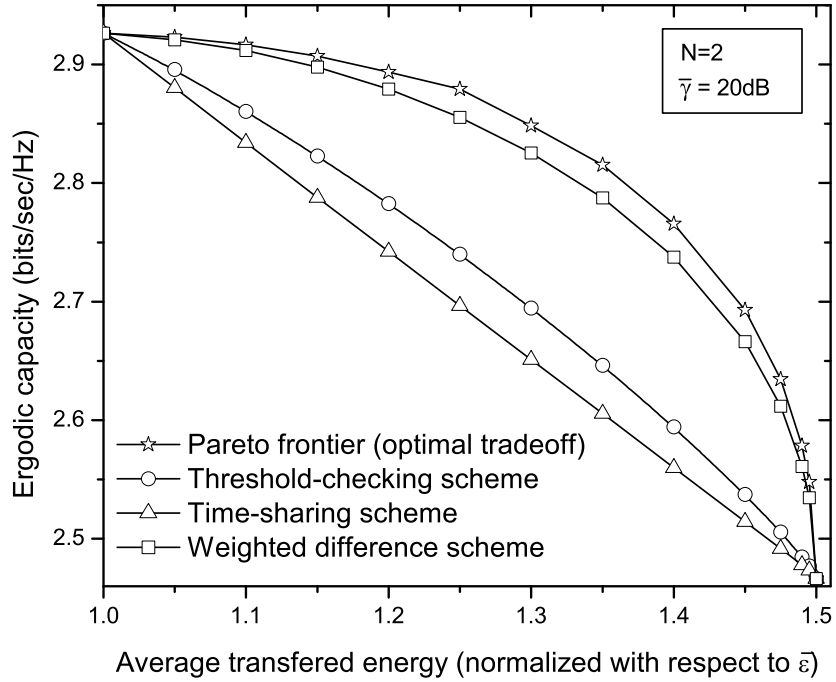


Fig. 3. The capacity-energy tradeoff of the schemes under consideration, for $\bar{\gamma} = 20$ dB.

the weighted difference scheme approaches the Pareto frontier in the region close to the tradeoff boundaries, and that it clearly outperforms the time-sharing and the threshold-checking schemes.

Similar observations are obtained from Fig. 4, where the same tradeoffs are now plotted vs. the tradeoff factor, δ , for $N = 2$ and $\bar{\gamma} = 10$ dB. We note that the weighted difference curve approximates the Pareto frontier for low $\bar{\gamma}$, for the entire range of δ . Moreover, the steepness of the curve in the region close to the boundaries reveals that a large gain in ergodic capacity (transferred energy) is attained without much sacrifice in energy transfer (ergodic capacity), for δ approaching zero or one. Furthermore, Fig. 4 shows that the theoretically derived tradeoff results pertaining to the schemes considered in Section III are in agreement with simulations.

The ergodic capacity vs. the average SNR per link, $\bar{\gamma}$, for several values of δ , is illustrated in Fig. 5. We observe that by increasing the tradeoff factor from $\delta = 0$ to $\delta = 1$, a capacity decrease occurs, which corresponds to an SNR loss of approximately 3 dB. That is, the cost in terms of capacity for increasing the wireless energy transfer to \mathcal{H} from its minimum to its maximum possible value is approximately 3 dB. This capacity cost is reduced if a tradeoff factor smaller than one is

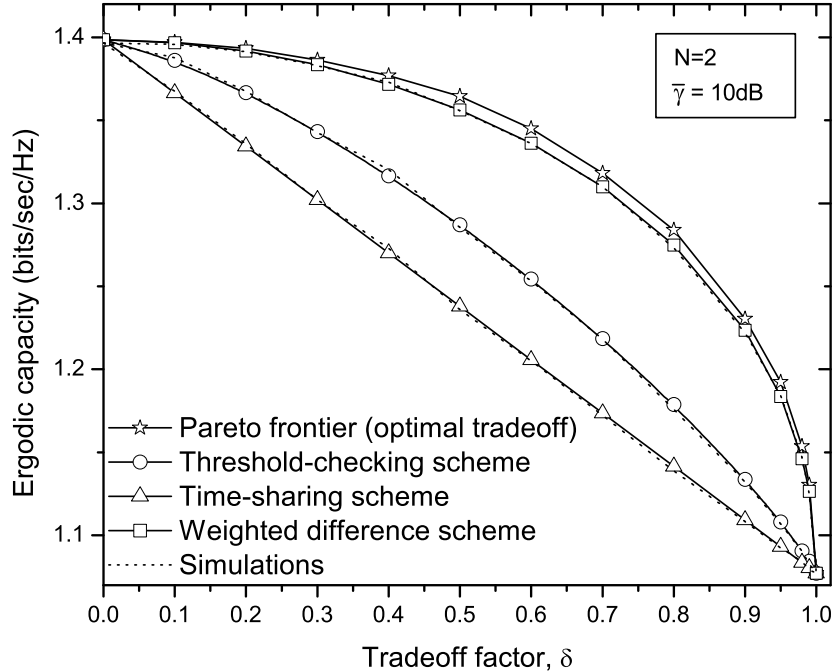


Fig. 4. The capacity-energy tradeoff of the schemes under consideration plotted vs. the tradeoff factor, for $\bar{\gamma} = 10$ dB.

selected. Moreover, we note that the capacity of the weighted difference scheme approximates that of the Pareto efficient scheme in (37); particularly for low SNRs, the weighted difference scheme is almost Pareto efficient.

B. Outage and No-Outage Probability vs. Energy Transfer

Fig. 6 illustrates the tradeoff between the probability of no-outage and the average energy transfer, for $N = 2$ and $\bar{\gamma} = 2\gamma_{\text{th}}/\ln(2)$. This particular choice for $\bar{\gamma}$ was made for convenience of presentation, since it follows from (10) that this choice of $\bar{\gamma}$ maximizes the range of the feasible tradeoff factor for the Pareto efficient scheme, yielding $\delta \in [0.5, 1]$. The main observations drawn from Fig. 6 are the following: a) The weighted difference scheme outperforms the threshold-checking and the time-sharing scheme, except for small values of δ . b) The threshold-checking scheme achieves Pareto efficiency for small δ , yet its performance is degraded for large δ , where it approaches the performance of the time-sharing scheme. c) The Pareto efficient scheme in (37) achieves the maximum feasible probability of no-outage at its lower boundary (i.e., for $\delta = 0.5$ for the case of $\bar{\gamma} = 2\gamma_{\text{th}}/\ln(2)$). The interpretation of this observation is as follows. It is trivial

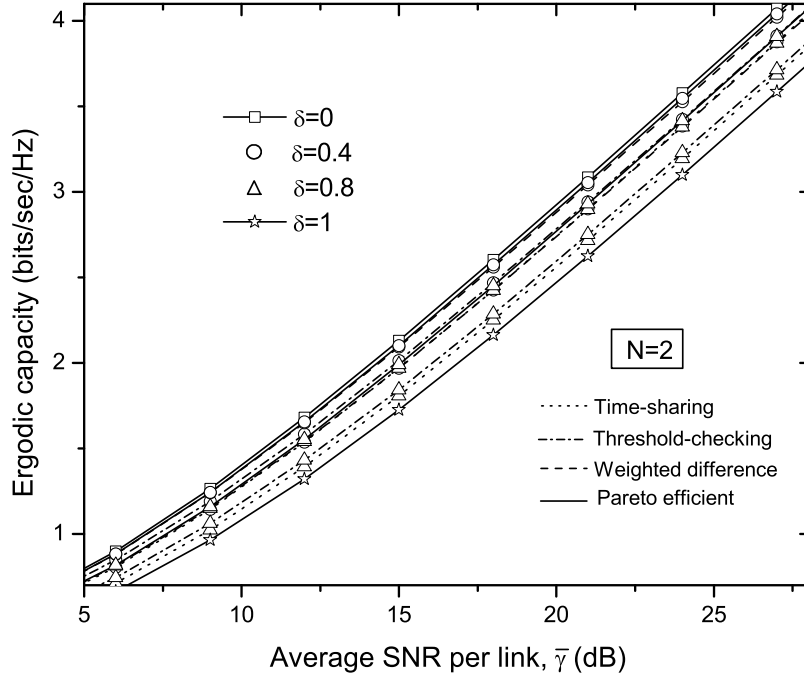


Fig. 5. Ergodic capacity vs. average SNR per link, $\bar{\gamma}$, for $N = 2$ and several values of the tradeoff factor, δ .

to prove that by using $\zeta = 0$ in (37) the optimum outage performance is achieved, since the relay selection is based solely on the ability to achieve an overall SNR larger than γ_{th} ; the energy transfer equals $\epsilon = \bar{\epsilon}$. However, observation c) reveals that by increasing ζ in (37) by an infinitesimally small amount, we can increase the transferred energy from $\bar{\epsilon}$ to $\bar{\epsilon} \left(\frac{3}{2} + e^{-\frac{4\gamma_{\text{th}}}{\bar{\gamma}}} - e^{-\frac{2\gamma_{\text{th}}}{\bar{\gamma}}} \right)$, as (41) suggests. In other words, we can offer more energy transfer to \mathcal{H} with no outage cost. In fact, this phenomenon stems from the on-off nature of the outage events.

The outage probability of the schemes under consideration are depicted in Fig. 7, for $N = 2$ and some values of δ (for the Pareto efficient scheme, if δ is smaller than its lower bound in (10) then this lower bound was used since the energy transfer to \mathcal{H} satisfies the required energy transfer that δ implies). The main conclusion drawn from Fig. 7 is that, as suggested by Corollary 4, the slope of the outage curves of the time-sharing, the threshold-checking, and the weighted difference schemes is negative unity (in a log-log scale) for $\delta \neq 0$, implying unit diversity order. However, the slope of the Pareto efficient scheme demonstrates full diversity order of $\mathcal{G}_d = 2$, unless the maximum tradeoff factor is allocated ($\delta = 1$). This result was also expected since for $\delta = 1$ the relay selection is made based solely on the strength of the $\mathcal{R}_i\text{-}\mathcal{H}$ channels. Moreover, we

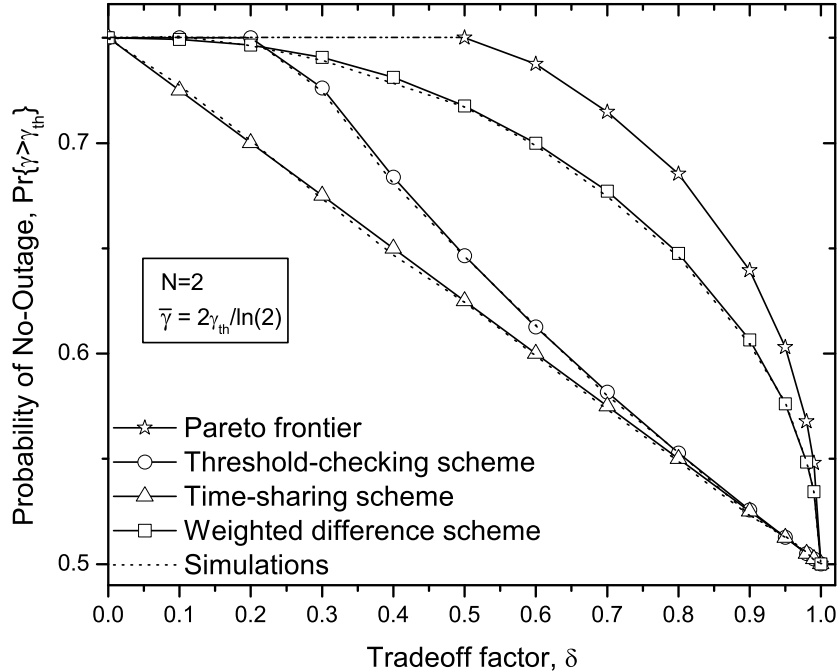


Fig. 6. The tradeoff between the probability of no-outage and the average energy transfer vs. the tradeoff factor, for $N = 2$ and $\bar{\gamma} = 2\gamma_{th}/\ln(2)$.

observe that the performance of the threshold-checking scheme is inferior to all its counterparts in the medium and high $\bar{\gamma}/\gamma_{th}$ region (equivalently, the medium and low outage probability region), a fact which corroborates Corollary 5. This behavior is in contrast to that in the low $\bar{\gamma}/\gamma_{th}$ region (i.e., for $\bar{\gamma}/\gamma_{th} < 5$ dB), where the threshold-checking scheme outperforms the time-sharing and the weighted-difference scheme, and actually approaches the behavior of the Pareto efficient scheme.

Finally, Fig. 8 deals with the case of three participating relays ($N = 3$), and shows the outage behavior of the time-sharing and the threshold-checking scheme. We observe that the time-sharing scheme outperforms the threshold-checking scheme for high values of $\bar{\gamma}/\gamma_{th}$, yet the threshold-checking scheme performs slightly better for low values of $\bar{\gamma}/\gamma_{th}$. Moreover, we notice that even the slightest increase of the required energy transfer to \mathcal{H} (as this is reflected by setting $\delta = 0.01$) severely deteriorates the asymptotic outage performance, corroborating thus Corollary 4. Nevertheless, the shift of the outage curves towards the negative unit slope occurs for relatively high SNRs for $\delta \rightarrow 0$, implying that the outage curves maintain their diversity characteristics in the medium SNR region when δ approaches zero.

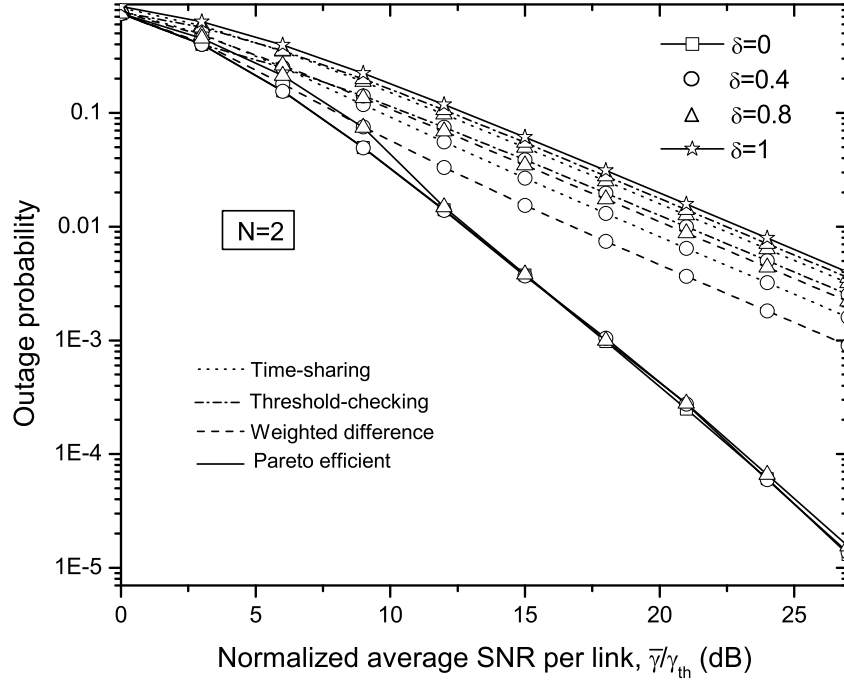


Fig. 7. Outage probability vs. normalized average SNR per link, $\bar{\gamma}/\gamma_{th}$, for $N = 2$ and several values of the tradeoff factor, δ .

VII. CONCLUSIONS

In scenarios involving relay-assisted information and energy transfer to a designated receiver and a designated RF energy harvester, respectively, the policy regarding the activated relay determines the tradeoff between quality of information transfer and wireless energy transfer. We provided a thorough analysis of this tradeoff for i.i.d. Rayleigh fading channels. For the versatile scenario of N candidate relays, “time-sharing selection” and “threshold-checking selection” schemes were developed and analyzed. Numerical results showed that “threshold-checking selection” is better in terms of achieved capacity for a given required energy transfer. However, in terms of outage probability for a given energy transfer, “time-sharing selection” outperforms “threshold-checking selection” when the normalized average SNR per link (with respect to the outage threshold SNR) is greater than 5 dB; for low SNRs, the outcome of the comparison is reversed.

For the special case of two candidate relays ($N = 2$), we developed the Pareto efficient relay selection policy. This policy yields the optimum capacity and outage probability for a given energy transfer, as well as the maximum energy transfer for a given constraint on the capacity or outage

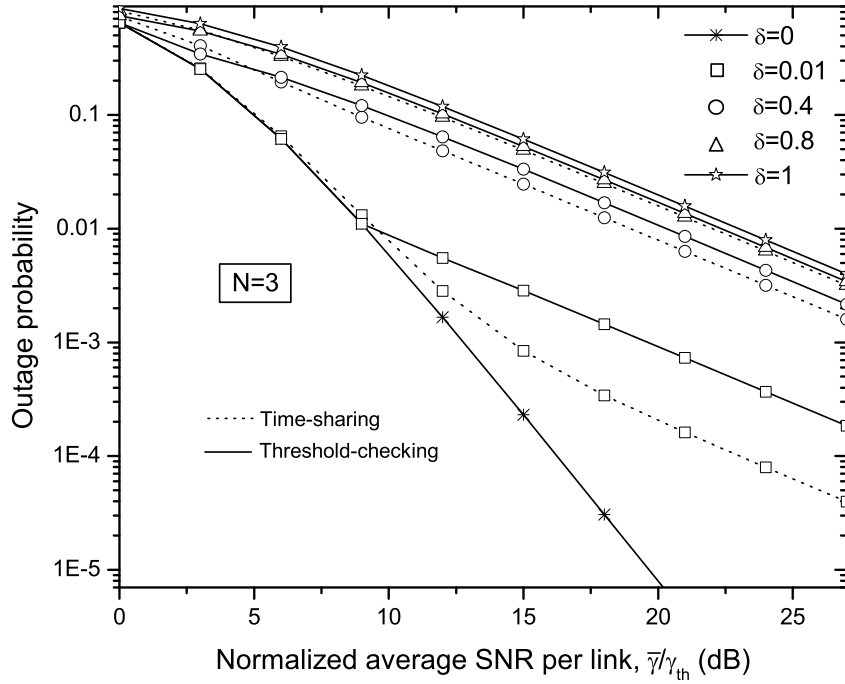


Fig. 8. Outage probability vs. normalized average SNR per link, $\bar{\gamma}/\gamma_{th}$, for $N = 3$ and several values of the tradeoff factor, δ .

probability. Along with the optimal policy, the selection scheme dubbed “weighted difference” was also proposed for $N = 2$. This scheme performs similarly to the Pareto efficient scheme, and yields tractable mathematical analysis. A general conclusion drawn from our analysis is that the diversity gain is lost when the links transferring energy to the RF harvester are included in the relay selection decision ($\delta > 0$), unless the Pareto efficient policy is employed and the links transferring information to the receiver are also included in the selection decision ($\delta < 1$). Moreover, the Pareto efficient scheme and the “weighted difference” scheme offer attractive tradeoffs when operating close to their upper and lower boundary ($\delta \approx 0$ and $\delta \approx 1$), in the sense that they achieve substantial improvement of capacity (and/or outage probability) with relatively little cost in energy transfer.

APPENDIX A

PROOF OF LEMMA 1

Clearly, the maximum ergodic capacity of the information transmission to \mathcal{D} equals the ergodic capacity of the $\mathcal{S}\text{-}\mathcal{R}_\kappa\text{-}\mathcal{D}$ link. For DF relaying, the information rate to \mathcal{D} is dominated by the bottleneck link, i.e., by the weakest of the $\mathcal{S}\text{-}\mathcal{R}_\kappa$ and $\mathcal{R}_\kappa\text{-}\mathcal{D}$ links. Thus, the maximum ergodic

capacity is obtained as

$$C_{\max} = \frac{1}{2} \int_0^{\infty} \log_2(1 + \gamma_{\kappa}) f_{\gamma_{\kappa}}(x) dx \quad (44)$$

where the pre-log factor $1/2$ is used because of the half-duplex assumption and $f_{\gamma_{\kappa}}(\cdot)$ denotes the probability density function (PDF) of $\gamma_{\kappa} = \max_{i=1, \dots, N} \gamma_i$. Since $\{\gamma_1, \gamma_2, \dots, \gamma_N\}$ is a set of exponentially distributed RVs, $f_{\gamma_{\kappa}}(\cdot)$ can be obtained from the theory of ordered statistics [24] and (2) as

$$f_{\gamma_{\kappa}}(x) = N \sum_{j=0}^{N-1} (-1)^j \binom{N-1}{j} \frac{2}{\bar{\gamma}} \exp\left(-2x \frac{j+1}{\bar{\gamma}}\right). \quad (45)$$

Plugging (45) into (44) and using integration by parts yields (7).

The minimum ergodic capacity occurs in the case where the CSI of the $\mathcal{S}\text{-}\mathcal{R}_i\text{-}\mathcal{D}$ links is not exploited for relay selection, or equivalently, when the relay is selected based on a process which is independent of the $\mathcal{S}\text{-}\mathcal{R}_i\text{-}\mathcal{D}$ channel strength². The minimum ergodic capacity is obtained directly from (7), by setting $N = 1$. In that case, (7) reduces to (6).

APPENDIX B

DERIVATION OF (17)

The first term in (17) is obtained by using (45) and employing integration by parts, yielding

$$\begin{aligned} E\{C_{\kappa} | \gamma_{\kappa} \geq \tau\} \Pr\{\gamma_{\kappa} \geq \tau\} &= \frac{\int_{\tau}^{\infty} \frac{1}{2} \log(1 + \gamma_{\kappa}) f_{\gamma_{\kappa}}(\gamma_{\kappa}) d\gamma_{\kappa}}{\Pr\{\gamma_{\kappa} \geq \tau\}} \Pr\{\gamma_{\kappa} \geq \tau\} \\ &= \sum_{j=0}^{N-1} \frac{N (-1)^j \binom{N-1}{j} e^{-\frac{2(j+1)\tau}{\bar{\gamma}}} \left[e^{\frac{2(j+1)(\tau+1)}{\bar{\gamma}}} \mathcal{E}_1\left(\frac{2(j+1)(\tau+1)}{\bar{\gamma}}\right) + \ln(\tau+1) \right]}{2(j+1) \ln(2)}. \end{aligned} \quad (46)$$

The second term in (17) is obtained as

$$E\{C_{\lambda} | \gamma_{\kappa} < \tau\} \Pr\{\gamma_{\kappa} < \tau\} = \sum_{i=1}^N \Pr\{s = i\} \frac{\int_0^{\tau} \frac{1}{2} \log_2(1+x) f_{\gamma_i}(x) dx}{\int_0^{\tau} f_{\gamma_i}(y) dy} \left(1 - e^{-\frac{2\tau}{\bar{\gamma}}}\right)^N. \quad (47)$$

Hence, using (2), (47) reduces to

$$E\{C_{\lambda} | \gamma_{\kappa} < \tau\} \Pr\{\gamma_{\kappa} < \tau\} = \frac{e^{\frac{2}{\bar{\gamma}}} \left[\mathcal{E}_1\left(\frac{2}{\bar{\gamma}}\right) - \mathcal{E}_1\left(\frac{2(1+\tau)}{\bar{\gamma}}\right) \right] - e^{-\frac{2\tau}{\bar{\gamma}}} \ln(1+\tau)}{2 \ln(2)} \left(1 - e^{-\frac{2\tau}{\bar{\gamma}}}\right)^{N-1}. \quad (48)$$

Adding (46) and (48) yields (17).

²In fact, the ergodic capacity can reach even lower values, if a relay that is known to have weak channel conditions is selected. This case, however, is not in line with the concept of opportunistic relay selection, and is therefore not considered here.

APPENDIX C

PROOF OF PROPOSITION 1

For analyzing the tradeoff of the weighted difference scheme, we distinguish the following four cases. The selected relay in each case follows directly from (21).

- *Case 1:* $\gamma_1 < \gamma_2$ and $\varepsilon_1 < \varepsilon_2$. *Selected relay:* $s = 2$.
- *Case 2:* $\gamma_1 < \gamma_2$ and $\varepsilon_1 > \varepsilon_2$. *Selected relay:* $s = 2$ if $\varepsilon_1 < \varepsilon_2 + (\gamma_2 - \gamma_1)/\nu$; $s = 1$ if $\varepsilon_1 > \varepsilon_2 + (\gamma_2 - \gamma_1)/\nu$.
- *Case 3:* $\gamma_1 > \gamma_2$ and $\varepsilon_1 < \varepsilon_2$. *Selected relay:* $s = 1$ if $\varepsilon_2 < \varepsilon_1 + (\gamma_1 - \gamma_2)/\nu$; $s = 2$ if $\varepsilon_2 > \varepsilon_1 + (\gamma_1 - \gamma_2)/\nu$.
- *Case 4:* $\gamma_1 > \gamma_2$ and $\varepsilon_1 > \varepsilon_2$. *Selected relay:* $s = 1$.

Considering the above cases, we can express the average energy transfer function of ν as

$$\begin{aligned}
\epsilon_{WD} = & \underbrace{\int_0^\infty f_{\gamma_1}(\gamma_1) \int_{\gamma_1}^\infty f_{\gamma_2}(\gamma_2) \int_0^\infty f_{\varepsilon_2}(\varepsilon_2) \int_0^{\varepsilon_2} \varepsilon_2 f_{\varepsilon_1}(\varepsilon_1) d\varepsilon_1 d\varepsilon_2 d\gamma_2 d\gamma_1}_{\mathcal{I}_1 \text{ (Case 1)}} \\
& + \underbrace{\int_0^\infty f_{\gamma_1}(\gamma_1) \int_{\gamma_1}^\infty f_{\gamma_2}(\gamma_2) \int_0^\infty f_{\varepsilon_2}(\varepsilon_2) \int_{\varepsilon_2}^{\varepsilon_2 + (\gamma_2 - \gamma_1)/\nu} \varepsilon_2 f_{\varepsilon_1}(\varepsilon_1) d\varepsilon_1 d\varepsilon_2 d\gamma_2 d\gamma_1}_{\mathcal{I}_{2a} \text{ (Case 2a)}} \\
& + \underbrace{\int_0^\infty f_{\gamma_1}(\gamma_1) \int_{\gamma_1}^\infty f_{\gamma_2}(\gamma_2) \int_0^\infty f_{\varepsilon_2}(\varepsilon_2) \int_{\varepsilon_2 + (\gamma_2 - \gamma_1)/\nu}^\infty \varepsilon_1 f_{\varepsilon_1}(\varepsilon_1) d\varepsilon_1 d\varepsilon_2 d\gamma_2 d\gamma_1}_{\mathcal{I}_{2b} \text{ (Case 2b)}} \\
& + \underbrace{\int_0^\infty f_{\gamma_1}(\gamma_1) \int_0^{\gamma_1} f_{\gamma_2}(\gamma_2) \int_0^\infty f_{\varepsilon_1}(\varepsilon_1) \int_{\varepsilon_1}^{\varepsilon_1 + (\gamma_1 - \gamma_2)/\nu} \varepsilon_1 f_{\varepsilon_2}(\varepsilon_2) d\varepsilon_2 d\varepsilon_1 d\gamma_2 d\gamma_1}_{\mathcal{I}_{3a} \text{ (Case 3a)}} \\
& + \underbrace{\int_0^\infty f_{\gamma_1}(\gamma_1) \int_0^{\gamma_1} f_{\gamma_2}(\gamma_2) \int_0^\infty f_{\varepsilon_1}(\varepsilon_1) \int_{\varepsilon_1 + (\gamma_1 - \gamma_2)/\nu}^\infty \varepsilon_2 f_{\varepsilon_2}(\varepsilon_2) d\varepsilon_2 d\varepsilon_1 d\gamma_2 d\gamma_1}_{\mathcal{I}_{3b} \text{ (Case 3b)}} \\
& + \underbrace{\int_0^\infty f_{\gamma_1}(\gamma_1) \int_0^{\gamma_1} f_{\gamma_2}(\gamma_2) \int_0^\infty f_{\varepsilon_2}(\varepsilon_2) \int_{\varepsilon_2}^\infty \varepsilon_1 f_{\varepsilon_1}(\varepsilon_1) d\varepsilon_1 d\varepsilon_2 d\gamma_2 d\gamma_1}_{\mathcal{I}_4 \text{ (Case 4)}}. \tag{49}
\end{aligned}$$

Using elementary integrations and [26, Eq. (3.351.7)], (49) reduces after algebraic manipulations to

$$\epsilon_{WD} = \underbrace{\frac{3}{8}\bar{\varepsilon}}_{\mathcal{I}_1} + \underbrace{\frac{\bar{\varepsilon}\bar{\gamma}}{8\bar{\gamma} + 16\nu\bar{\varepsilon}}}_{\mathcal{I}_{2a}} + \underbrace{\frac{\bar{\varepsilon}^2\nu(5\bar{\gamma} + 6\nu\bar{\varepsilon})}{4(\bar{\gamma} + 2\nu\bar{\varepsilon})^2}}_{\mathcal{I}_{2b}} + \underbrace{\frac{\bar{\varepsilon}\bar{\gamma}}{8\bar{\gamma} + 16\nu\bar{\varepsilon}}}_{\mathcal{I}_{3a}} + \underbrace{\frac{\bar{\varepsilon}^2\nu(5\bar{\gamma} + 6\nu\bar{\varepsilon})}{4(\bar{\gamma} + 2\nu\bar{\varepsilon})^2}}_{\mathcal{I}_{3b}} + \underbrace{\frac{3}{8}\bar{\varepsilon}}_{\mathcal{I}_4}$$

$$= \frac{\bar{\epsilon}}{2} \left[3 - \frac{\bar{\gamma}^2}{(\bar{\gamma} + 2\nu\bar{\epsilon})^2} \right]. \quad (50)$$

It is interesting to observe from (50) the following: $\mathcal{I}_1 = \mathcal{I}_4$; $\mathcal{I}_{2a} = \mathcal{I}_{3a}$; $\mathcal{I}_{2b} = \mathcal{I}_{3b}$; \mathcal{I}_1 and \mathcal{I}_4 are independent of $\bar{\gamma}$. All the above observations are explained by the assumption that all participating channels are i.i.d. Solving (50) with respect to ν yields

$$\nu = \frac{\bar{\gamma}}{2\bar{\epsilon}} \left(\sqrt{\frac{\bar{\epsilon}}{3\bar{\epsilon} - 2\epsilon_{WD}}} - 1 \right), \quad \bar{\epsilon} \leq \epsilon_{WD} \leq H_2\bar{\epsilon}. \quad (51)$$

The ergodic capacity of the weighted difference scheme is calculated in a way similar to the average transferred energy. Considering again *Case 1 - Case 4*, yields

$$\begin{aligned} C_{WD} = & \underbrace{\int_0^\infty f_{\gamma_1}(\gamma_1) \int_{\gamma_1}^\infty f_{\gamma_2}(\gamma_2) \int_0^\infty f_{\epsilon_2}(\epsilon_2) \int_0^{\epsilon_2} \frac{\log_2(1+\gamma_2)}{2} f_{\epsilon_1}(\epsilon_1) d\epsilon_1 d\epsilon_2 d\gamma_2 d\gamma_1}_{\mathcal{J}_1 \text{ (Case 1)}} \\ & + \underbrace{\int_0^\infty f_{\gamma_1}(\gamma_1) \int_{\gamma_1}^\infty f_{\gamma_2}(\gamma_2) \int_0^\infty f_{\epsilon_2}(\epsilon_2) \int_{\epsilon_2}^{\epsilon_2+(\gamma_2-\gamma_1)/\nu} \frac{\log_2(1+\gamma_2)}{2} f_{\epsilon_1}(\epsilon_1) d\epsilon_1 d\epsilon_2 d\gamma_2 d\gamma_1}_{\mathcal{J}_{2a} \text{ (Case 2a)}} \\ & + \underbrace{\int_0^\infty f_{\gamma_1}(\gamma_1) \int_{\gamma_1}^\infty f_{\gamma_2}(\gamma_2) \int_0^\infty f_{\epsilon_2}(\epsilon_2) \int_{\epsilon_2+(\gamma_2-\gamma_1)/\nu}^\infty \frac{\log_2(1+\gamma_1)}{2} f_{\epsilon_1}(\epsilon_1) d\epsilon_1 d\epsilon_2 d\gamma_2 d\gamma_1}_{\mathcal{J}_{2b} \text{ (Case 2b)}} \\ & + \underbrace{\int_0^\infty f_{\gamma_1}(\gamma_1) \int_0^{\gamma_1} f_{\gamma_2}(\gamma_2) \int_0^\infty f_{\epsilon_1}(\epsilon_1) \int_{\epsilon_1}^{\epsilon_1+(\gamma_1-\gamma_2)/\nu} \frac{\log_2(1+\gamma_1)}{2} f_{\epsilon_2}(\epsilon_2) d\epsilon_2 d\epsilon_1 d\gamma_2 d\gamma_1}_{\mathcal{J}_{3a} \text{ (Case 3a)}} \\ & + \underbrace{\int_0^\infty f_{\gamma_1}(\gamma_1) \int_0^{\gamma_1} f_{\gamma_2}(\gamma_2) \int_0^\infty f_{\epsilon_1}(\epsilon_1) \int_{\epsilon_1+(\gamma_1-\gamma_2)/\nu}^\infty \frac{\log_2(1+\gamma_2)}{2} f_{\epsilon_2}(\epsilon_2) d\epsilon_2 d\epsilon_1 d\gamma_2 d\gamma_1}_{\mathcal{J}_{3b} \text{ (Case 3b)}} \\ & + \underbrace{\int_0^\infty f_{\gamma_1}(\gamma_1) \int_0^{\gamma_1} f_{\gamma_2}(\gamma_2) \int_0^\infty f_{\epsilon_2}(\epsilon_2) \int_{\epsilon_2}^\infty \frac{\log_2(1+\gamma_1)}{2} f_{\epsilon_1}(\epsilon_1) d\epsilon_1 d\epsilon_2 d\gamma_2 d\gamma_1}_{\mathcal{J}_4 \text{ (Case 4)}}. \quad (52) \end{aligned}$$

Using integration by parts where appropriate, in conjunction with [26, Eq. (3.351.7)] and [26, Eq. (4.337.2)], (52) reduces after algebraic manipulations to

$$\begin{aligned} C_{WD} = & 2 \underbrace{\frac{2e^{\frac{2}{\bar{\gamma}}}\mathcal{E}_1\left(\frac{2}{\bar{\gamma}}\right) - e^{\frac{4}{\bar{\gamma}}}\mathcal{E}_1\left(\frac{4}{\bar{\gamma}}\right)}{8\ln(2)}}_{\mathcal{J}_1 \text{ (}\mathcal{J}_4\text{)}} \\ & + 2 \underbrace{\frac{2(\bar{\gamma}^2 - 4\nu^2\bar{\epsilon}^2)\mathcal{E}_1\left(\frac{2}{\bar{\gamma}}\right) + 8e^{\frac{1}{\nu\bar{\epsilon}}}\nu^2\bar{\epsilon}^2\mathcal{E}_1\left(\frac{2}{\bar{\gamma}} + \frac{1}{\nu\bar{\epsilon}}\right) - e^{\frac{2}{\bar{\gamma}}}(\bar{\gamma}^2 + 4\nu^2\bar{\epsilon}^2)\mathcal{E}_1\left(\frac{4}{\bar{\gamma}}\right)}{8e^{-\frac{2}{\bar{\gamma}}}(\bar{\gamma}^2 - 4\nu^2\bar{\epsilon}^2)\ln(2)}}_{\mathcal{J}_2 \text{ (}\mathcal{J}_3\text{)}} \quad (53) \end{aligned}$$

$$= \frac{2(\bar{\gamma}^2 - 4\nu^2\bar{\varepsilon}^2)\mathcal{E}_1\left(\frac{2}{\bar{\gamma}}\right) + 4e^{\frac{1}{\nu\bar{\varepsilon}}}\nu^2\bar{\varepsilon}^2\mathcal{E}_1\left(\frac{2}{\bar{\gamma}} + \frac{1}{\nu\bar{\varepsilon}}\right) - e^{\frac{2}{\bar{\gamma}}}\bar{\gamma}^2\mathcal{E}_1\left(\frac{4}{\bar{\gamma}}\right)}{2e^{-\frac{2}{\bar{\gamma}}}(\bar{\gamma}^2 - 4\nu^2\bar{\varepsilon}^2)\ln(2)} \quad (54)$$

where the factor 2 in front of each of the two terms in (53) is due to symmetry, similar to the observations in (50). Plugging (51) into (54) yields (22).

APPENDIX D

PROOF OF PROPOSITION 2

The outage probability of the weighted difference scheme is obtained by utilizing the four cases considered in Appendix C, as follows

$$\begin{aligned}
P_{out,WD} &= \underbrace{\int_0^{\gamma_{th}} f_{\gamma_2}(\gamma_2) \int_0^{\gamma_2} f_{\gamma_1}(\gamma_1) \int_0^\infty f_{\varepsilon_2}(\varepsilon_2) \int_0^{\varepsilon_2} f_{\varepsilon_1}(\varepsilon_1) d\varepsilon_1 d\varepsilon_2 d\gamma_1 d\gamma_2}_{\mathcal{K}_1 \text{ (Case 1)}} \\
&+ \underbrace{\int_0^{\gamma_{th}} f_{\gamma_2}(\gamma_2) \int_0^{\gamma_2} f_{\gamma_1}(\gamma_1) \int_0^\infty f_{\varepsilon_2}(\varepsilon_2) \int_{\varepsilon_2}^{\varepsilon_2+(\gamma_2-\gamma_1)/\nu} f_{\varepsilon_1}(\varepsilon_1) d\varepsilon_1 d\varepsilon_2 d\gamma_1 d\gamma_2}_{\mathcal{K}_{2a} \text{ (Case 2a)}} \\
&+ \underbrace{\int_0^{\gamma_{th}} f_{\gamma_1}(\gamma_1) \int_{\gamma_1}^\infty f_{\gamma_2}(\gamma_2) \int_0^\infty f_{\varepsilon_2}(\varepsilon_2) \int_{\varepsilon_2+(\gamma_2-\gamma_1)/\nu}^\infty f_{\varepsilon_1}(\varepsilon_1) d\varepsilon_1 d\varepsilon_2 d\gamma_2 d\gamma_1}_{\mathcal{K}_{2b} \text{ (Case 2b)}} \\
&+ \underbrace{\int_0^{\gamma_{th}} f_{\gamma_1}(\gamma_1) \int_0^{\gamma_1} f_{\gamma_2}(\gamma_2) \int_0^\infty f_{\varepsilon_1}(\varepsilon_1) \int_{\varepsilon_1}^{\varepsilon_1+(\gamma_1-\gamma_2)/\nu} f_{\varepsilon_2}(\varepsilon_2) d\varepsilon_2 d\varepsilon_1 d\gamma_2 d\gamma_1}_{\mathcal{K}_{3a} \text{ (Case 3a)}} \\
&+ \underbrace{\int_0^{\gamma_{th}} f_{\gamma_2}(\gamma_2) \int_{\gamma_2}^\infty f_{\gamma_1}(\gamma_1) \int_0^\infty f_{\varepsilon_1}(\varepsilon_1) \int_{\varepsilon_1+(\gamma_1-\gamma_2)/\nu}^\infty f_{\varepsilon_2}(\varepsilon_2) d\varepsilon_2 d\varepsilon_1 d\gamma_1 d\gamma_2}_{\mathcal{K}_{3b} \text{ (Case 3b)}} \\
&+ \underbrace{\int_0^{\gamma_{th}} f_{\gamma_1}(\gamma_1) \int_0^{\gamma_1} f_{\gamma_2}(\gamma_2) \int_0^\infty f_{\varepsilon_2}(\varepsilon_2) \int_{\varepsilon_2}^\infty f_{\varepsilon_1}(\varepsilon_1) d\varepsilon_1 d\varepsilon_2 d\gamma_2 d\gamma_1}_{\mathcal{K}_4 \text{ (Case 4)}}. \quad (55)
\end{aligned}$$

Working similarly as in Appendix C, we can simplify (55) to

$$\begin{aligned}
P_{out,WD} &= 2 \underbrace{\frac{1}{4} e^{-\frac{4\gamma_{th}}{\bar{\gamma}}} \left(e^{\frac{2\gamma_{th}}{\bar{\gamma}}} - 1 \right)^2}_{\mathcal{K}_1(\mathcal{K}_4)} + 2 \underbrace{\left\{ \frac{1}{4} + e^{-\frac{4\gamma_{th}}{\bar{\gamma}}} \left[\frac{\bar{\gamma}^2 + 4\nu^2\bar{\varepsilon}^2}{\bar{\gamma}^2 - 4\nu^2\bar{\varepsilon}^2} - 2e^{\frac{2\gamma_{th}}{\bar{\gamma}}} \left(1 + \frac{4e^{-\frac{\gamma_{th}}{\nu\bar{\varepsilon}}}\nu^2\bar{\varepsilon}^2}{\bar{\gamma}^2 - 4\nu^2\bar{\varepsilon}^2} \right) \right] \right\}}_{\mathcal{K}_2(\mathcal{K}_3)} \\
&= \frac{e^{-\frac{4\gamma_{th}}{\bar{\gamma}}} \left(e^{\frac{2\gamma_{th}}{\bar{\gamma}}} - 1 \right)^2 \bar{\gamma}^2 + 4\nu^2\bar{\varepsilon}^2 \left[e^{-\frac{2\gamma_{th}}{\bar{\gamma}}} \left(2 - e^{-\frac{\gamma_{th}}{\nu\bar{\varepsilon}}} \right) - 1 \right]}{\bar{\gamma}^2 - 4\nu^2\bar{\varepsilon}^2}. \quad (56)
\end{aligned}$$

Substituting (51) in (56) yields the outage probability of the weighted difference scheme expressed as a function of ϵ_{WD} and $\bar{\epsilon}$, as shown in (29). Using (10), (30) is derived from (29).

APPENDIX E

PROOF OF THEOREM 1

By its definition, \mathcal{F} represents the average of a performance metric over a window of M transmission sessions, when $M \rightarrow \infty$. In order to mathematically express the selection of either \mathcal{R}_1 or \mathcal{R}_2 in a given transmission session, m , we introduce the binary auxiliary variable w_m , such that $w_m = 1$ if $s = 1$; $w_m = 0$ if $s = 2$. Then, the problem of maximizing \mathcal{F} for given energy transfer constraints is expressed as

$$\begin{aligned} & \max_{w_m} \lim_{M \rightarrow \infty} \frac{1}{M} \sum_{m=1}^M [w_m \mathcal{F}(\gamma_{1,m}) + (1 - w_m) \mathcal{F}(\gamma_{2,m})] \\ \text{s.t.} \quad & \frac{1}{M} \sum_{m=1}^M w_m (1 - w_m) = 0 \\ & \lim_{M \rightarrow \infty} \frac{1}{M} \sum_{m=1}^M [w_m \epsilon_{1,m} + (1 - w_m) \epsilon_{2,m}] \geq \epsilon \end{aligned} \quad (57)$$

where $\{\gamma_{1,m}, \epsilon_{1,m}\}$, $\{\gamma_{2,m}, \epsilon_{2,m}\}$ denote the {SNR, harvested energy} of the $\mathcal{S}\text{-}\mathcal{R}_1\text{-}\mathcal{D}$ and $\mathcal{S}\text{-}\mathcal{R}_2\text{-}\mathcal{D}$ links, respectively, in transmission frame m . Using the parameters ξ_m and ζ as non-negative Lagrange multipliers, the Lagrangian of the above problem is obtained as

$$\begin{aligned} \mathcal{L} = & \lim_{M \rightarrow \infty} \frac{1}{M} \sum_{m=1}^M [w_m \mathcal{F}(\gamma_{1,m}) + (1 - w_m) \mathcal{F}(\gamma_{2,m})] \\ & + \frac{\xi_m}{M} \sum_{m=1}^M w_m (1 - w_m) + \lim_{M \rightarrow \infty} \frac{\zeta}{M} \sum_{m=1}^M [w_m \epsilon_{1,m} + (1 - w_m) \epsilon_{2,m} - \epsilon]. \end{aligned} \quad (58)$$

Let us not concentrate on maximizing \mathcal{L} for a given transmission frame m , and let us drop the index m for notational simplicity. The derivative of \mathcal{L} with respect to w is obtained from (58) as

$$\frac{\partial \mathcal{L}}{\partial w} = \frac{1}{M} \mathcal{F}(\gamma_1) - \frac{1}{M} \mathcal{F}(\gamma_2) + \frac{\xi}{M} (1 - 2w) + \frac{\zeta}{M} (\epsilon_1 - \epsilon_2). \quad (59)$$

Setting the derivative in (59) equal to zero and solving with respect to w yields

$$w = \frac{\Delta \mathcal{F} + \zeta \Delta \epsilon + \xi}{2\xi} \quad (60)$$

where Δ denotes difference, such that $\Delta\mathcal{F} = \mathcal{F}(\gamma_1) - \mathcal{F}(\gamma_2)$ and $\Delta\varepsilon = \varepsilon_1 - \varepsilon_2$. Since w is a binary variable (i.e., it equals either zero or one), (60) yields

$$w = \begin{cases} 0, & \text{if } \xi = -\Delta\mathcal{F} - \zeta \Delta\varepsilon \\ 1, & \text{if } \xi = \Delta\mathcal{F} + \zeta \Delta\varepsilon \end{cases}. \quad (61)$$

Considering that $\xi \geq 0$, (61) yields the optimal relay selection rule given the value of $\zeta \geq 0$, as follows

$$w = \begin{cases} 0, & \text{if } \Delta\mathcal{F} + \zeta \Delta\varepsilon < 0 \\ 1, & \text{if } \Delta\mathcal{F} + \zeta \Delta\varepsilon \geq 0 \end{cases}. \quad (62)$$

which is equivalent to (37). Since $\mathcal{F}(\gamma_i)$ is a non-decreasing function of γ_i , the policy in (37) also maximizes the average energy transfer for a given \mathcal{F} . This completes the proof.

REFERENCES

- [1] G. Fettweis and E. Zimmermann, "ICT energy consumption, trends and challenges," in *Proc. of International Symposium on Wireless Personal Multimedia Communications*, 2008.
- [2] "Cisco visual networking index: Forecast and methodology, 2011-2016, white paper," [Online]. Available: http://www.cisco.com/en/US/solutions/collateral/ns341/ns525/ns537/ns705/ns827/white_paper_c11-481360.pdf.
- [3] E. Hossain, V. K. Bhargava, and G. P. Fettweis, *Green Radio Communication Networks*. New York: Cambridge University Press, 2012.
- [4] Z. Hasan, H. Boostanimehr, and V. K. Bhargava, "Green cellular networks: A survey, some research issues and challenges," *IEEE Communications Surveys & Tutorials*, pp. 524–540, Fourth Quarter 2011.
- [5] B. Medepally and N. Mehta, "Voluntary energy harvesting relays and selection in cooperative wireless networks," *IEEE Trans Wireless Commun.*, pp. 3543–3553, Nov. 2010.
- [6] C. K. Ho and R. Zhang, "Optimal energy allocation for wireless communications with energy harvesting constraints," *IEEE Trans. Signal Process.*, pp. 4808–4818, Sep. 2012.
- [7] O. Ozel, K. Tutuncuoglu, J. Yang, S. Ulukus, and A. Yener, "Transmission with energy harvesting nodes in fading wireless channels: Optimal policies," *IEEE J. Sel. Areas Commun.*, vol. 29, pp. 1732–1743, Sep. 2011.
- [8] S. Sudevalayam and P. Kulkarni, "Energy harvesting sensor nodes: Survey and implications," *IEEE Communications Surveys & Tutorials*, pp. 443–461, Third Quarter 2011.
- [9] A. A. Nasir, X. Zhou, S. Durrani, and R. A. Kennedy, "Relaying protocols for wireless energy harvesting and information processing," 2012, submitted for possible publication in *IEEE Trans. Wireless Commun.* [Online]. Available: <http://arxiv.org/abs/1212.5406>.
- [10] K. Huang and V. K. N. Lau, "Enabling wireless power transfer in cellular networks: Architecture, modelling and deployment," 2012, submitted for possible publication in *IEEE Trans. Wireless Commun.* [Online]. Available: <http://arxiv.org/abs/1105.4999>.
- [11] "Powercast chipset and RF energy harvesting reference design enable low-cost wireless power over distance," Powercast Corporation, 2012. [Online] Available: <http://www.powercastco.com/powercasts-chipset-and-rf-energy-harvesting-reference-design-enable-low-cost-wireless-power-over-distance-20120222/>.

- [12] I. Krikidis, S. Timotheou, and S. Sasaki, "RF energy transfer for cooperative networks: Data relaying or energy harvesting?" *IEEE Commun. Lett.*, vol. 16, pp. 1772–1775, Nov. 2012.
- [13] L. R. Varshney, "Transporting information and energy simultaneously," in *Proc. of IEEE International Symposium on Information Theory (ISIT)*, Toronto, Canada, Jul. 2008, pp. 1612–1616.
- [14] P. Grover and A. Sahai, "Shannon meets Tesla: Wireless information and power transfer," in *Proc. of IEEE International Symposium on Information Theory (ISIT)*, Austin, TX, Jun. 2010, pp. 2363–2367.
- [15] C. Shen, W. C. Li, and T. H. Chang, "Simultaneous information and energy transfer: A two-user MISO interference channel case," in *Proc. of IEEE Global Communications Conference (Globecom)*, Anaheim, CA, Dec. 2012, pp. 3886–3891.
- [16] R. Zhang and C. K. Ho, "MIMO broadcasting for simultaneous wireless information and power transfer," *IEEE Trans. Wireless Commun.*, 2012, accepted for publication. [Online]. Available: <http://arxiv.org/abs/1105.4999>.
- [17] B. K. Chalise, Y. D. Zhang, and M. G. Amin, "Energy harvesting in an OSTBC based amplify-and-forward relay system," in *Proc. of IEEE International Conference on Acoustics, Speech and Signal Processing (ICASSP)*, Kyoto, Japan, Mar. 2012, pp. 3201–3204.
- [18] K. Ishibashi, H. Ochiai, and V. Tarokh, "Energy harvesting cooperative communications," in *Proc. of IEEE International Symposium on Personal, Indoor, and Mobile Radio Communications (PIMRC)*, Sydney, Australia, Sep. 2012, pp. 1819–1823.
- [19] M. Dohler, *Cooperative Communications: Hardware, Channel and PHY*, 1st ed. New York, NY: Wiley, 2010.
- [20] F. H. Fitzek and E. M. D. Katz, *Cooperation in Wireless Networks: Principles and Applications*, 1st ed. Dordrecht, Netherlands: Springer, 2007.
- [21] B. Maham, A. Behnad, and M. Debbah, "Analysis of outage probability and throughput for half-duplex hybrid-ARQ relay channels," *IEEE Trans. Veh. Technol.*, vol. 61, pp. 3061–3070, Sep. 2012.
- [22] R. M. Starr, *General Equilibrium Theory: An Introduction*. Cambridge University Press, 1997.
- [23] M. Abramovitz and I. A. Stegun, *Handbook of Mathematical Functions with Formulas, Graphs, and Mathematical Tables*, 9th ed. New York: Dover, 1972.
- [24] H. A. David and H. N. Nagaraja, *Order Statistics*, 3rd ed. New York: Wiley, 2003.
- [25] Z. Wang and G. B. Giannakis, "A simple and general parameterization quantifying performance in fading channels," *IEEE Trans. Commun.*, vol. 51, pp. 1389–1398, Aug. 2003.
- [26] I. S. Gradshteyn and I. M. Ryzhik, *Table of Integrals, Series, and Products*, 6th ed. New York: Academic, 2000.